



**Yu-Shiba-Rusinov states, BCS-BEC crossover, and exact solution in the flat-band limit**R. Žitko  and L. Pavešič *Jožef Stefan Institute, Jamova 39, SI-1000 Ljubljana, Slovenia  
and Faculty of Mathematics and Physics, University of Ljubljana, Jadranska 19, SI-1000 Ljubljana, Slovenia*

(Received 28 April 2022; revised 20 June 2022; accepted 12 July 2022; published 20 July 2022)

We study the subgap Yu-Shiba-Rusinov (YSR) states in the Richardson's model of a superconductor with a magnetic impurity for different electron pairing strengths from the weak-coupling Bardeen-Cooper-Schrieffer (BCS) regime to the strong-coupling Bose-Einstein-condensate (BEC) regime. We observe that the effect of the increasing pairing strength on the YSR excitation spectrum as a function of hybridization strength and impurity onsite potential is only quantitative and, in fact, rather weak when the results are appropriately rescaled. We furthermore show that the problem is analytically solvable in the deep BEC limit which is equivalent to flat-band superconductivity. This exact solution can be related to a zero-bandwidth (ZBW) effective BCS mean-field Hamiltonian where the superconductor is described by a single electron level with onsite pairing. The small difference between the BCS and BEC regimes of the Richardson's model explains the success of the simple ZBW calculations for BCS mean-field Hamiltonians. A ZBW model requires only a suitable parameter rescaling to become useful as a quantitative predictive tool for the full problem.

DOI: [10.1103/PhysRevB.106.024513](https://doi.org/10.1103/PhysRevB.106.024513)**I. INTRODUCTION**

The pairing interaction is a key concept in nuclear and solid-state physics, as well as in quantum many-body theory in general. Pairing between fermions has been studied in bulk materials [1–3], thin films [4], layered materials [5–7], atomic nuclei [8–12], nuclear matter in neutron stars [13], cold atom systems [14–19], nanoscopic metal grains [20–24], and ultra-small superconducting islands [25,26]. When the pairing is weak, the BCS mean-field approach works well [1]. When the pairing is strong, all fermionic particles pair up into bosons, then the bosons condense: this produces a BEC. Both regimes are smoothly connected, despite the fact that the two limits are physically quite different [14,19,27].

A magnetic impurity, such as a magnetic dopant or a semiconductor quantum dot (QD), is well known to induce subgap states in the superconducting gap of a BCS superconductor [28–39], which are known as the Yu-Shiba-Rusinov (YSR) states in the limit of well-defined local moment. This raises the questions about the persistence of the YSR states all the way to the BEC limit and about the evolution of their properties in this cross-over. These questions are pertinent because the ground state and the elementary excitations in the two limits have different properties [19].

In this work, we address this subject by coupling a magnetic impurity to a superconductor (SC) described by the Richardson's "picket-fence" pairing model, and tracking the subgap states through the crossover from weak to strong pairing. We show that the YSR states not only persist in the cross-over from the BCS to the BEC regime, but do not even change significantly at the quantitative level after an appropriate rescaling of the input parameters and the resulting energies. We also establish that a simple model based on the flat-band limit of the Richardson's model (RM) reproduces

the full phenomenology of an interacting QD coupled to a SC island.

The subject of Shiba states across the BEC-BCS crossover has been recently studied in the context of cold-atom systems using a continuous-space Hamiltonian with a contact atom-atom interaction, a static impurity with no internal quantum dynamics, and making use of a mean-field level of approximation in all regimes [40]. In that model, the YSR state does not exist for all parameters across the transition and a reentrant behavior was found instead. Due to the significant differences between the QD-SC setup and the impurity in atomic cloud, these two Hamiltonians represent two very different problems that cannot be compared in a sensible way. In this work we address only the former problem.

The RM first appeared as a model of pairing forces in nuclear physics [11,41,42] and was later reintroduced as a description of nanoscale SC grains [24,43–45]. The SC is modeled as a set of equidistant energy levels representing the time-reversal conjugate single-particle states with all-to-all pairing interaction. While the RM exactly reduces to a BCS model in the thermodynamic limit, it has important advantages for smaller systems. Namely, it does not use the mean-field approximation and thus conserves particle number. This makes it a more suitable choice for the modeling of mesoscopic SC systems. Unlike BCS, it is also applicable at all coupling strengths [46] which is critical in the present work.

The RM is integrable and analytically solvable in terms of hard-core bosons [11,42], but coupling it with an impurity level introduces pair-breaking processes and breaks integrability. We have previously found a representation of the QD-SC model as a matrix product operator (MPO), allowing us to use density matrix renormalization group (DMRG) [47–49] to obtain exact solutions for a QD coupled to one [50] or two [51] SC channels. With this method we

obtain exact properties of a magnetic impurity coupled to an interacting SC with no parameter restrictions, from the BCS to the BEC limits, for all system sizes including ultrasmall SC islands. Good agreement to experiment confirms that this is a suitable description of real systems [52].

This article is organized as follows. In Sec. II we present the Hamiltonian and the methods that permit its numerical solution. In Sec. III we present the results for the evolution from the BCS to the BEC limit. In Sec. IV we present an exact solution of the model in the limit of a completely flat band (equivalent to the deep BEC regime). In Sec. V we discuss how this solution can also be considered as arising from a ZBW BCS model which leads to exactly the same matrix representation. We conclude in Sec. VI with a perspective on the possible extensions of the flat-band model, e.g., to a two-channel (Josephson junction) situation. Some lengthy derivations are presented in Appendices A–C. In the Supplemental Material we provide Mathematica notebooks with a computer-algebra verification of all mathematical statements presented in this work [53]. The full source code of the DMRG solver is available on a public repository, including a large set of examples [54]. We also provide the input files for the solver and a corresponding Mathematica notebook with an exact calculation of the ground state energies in the flat-band limit [53]; this reference calculation is discussed in Appendix D.

## II. MODEL AND METHOD

The Richardson's model is [24,50]

$$H = \sum_{i\sigma} \epsilon_i c_{i\sigma}^\dagger c_{i\sigma} - G \sum_{i,j} c_{i\uparrow}^\dagger c_{i\downarrow}^\dagger c_{j\downarrow} c_{j\uparrow}, \quad (1)$$

where  $c_{i\sigma}^\dagger$  creates a particle in the level  $i$  with spin  $\sigma \in \{\uparrow, \downarrow\}$  and  $\epsilon_i$  are the energy levels spanning the interval  $[-D : D]$  spaced by  $d = 2D/\mathcal{L}$ , where the half-bandwidth  $D \equiv 1$  sets the energy scale, and  $\mathcal{L}$  is the total number of levels. The indexes  $i$  and  $j$  range from 1 to  $\mathcal{L}$ . The coupling  $G$  can also be written as

$$G = \alpha d = D \frac{2\alpha}{\mathcal{L}} = \frac{g}{\mathcal{L}}, \quad (2)$$

where we have introduced  $\alpha$  as the dimensionless strength of the pairing interaction, and  $g$  as the corresponding dimension-full strength;  $\alpha$  and  $g$  are intensive quantities.

The BCS to BEC limiting process can be implemented in two equivalent ways: by increasing the coupling  $G$  at constant bandwidth  $D$ , or by decreasing the bandwidth  $D$  at constant coupling  $G$ . We opt for the second possibility in this work. We implement this by appropriately rescaling the coefficients  $\epsilon_i$  in the kinetic-energy term of the SC Hamiltonian. We introduce  $\gamma$  as a parameter that multiplies the kinetic energy term of the Hamiltonian. Going to the BEC limit thus corresponds to taking the flat-band limit ( $\gamma \rightarrow 0$ ), i.e., omitting the kinetic-energy terms from the Hamiltonian.

We describe the coupling of the interacting QD to the SC using an Anderson impurity Hamiltonian [50,55–57]:

$$\begin{aligned} H_{\text{QD}} &= \epsilon \hat{n} + U \hat{n}_\uparrow \hat{n}_\downarrow + v \frac{1}{\sqrt{\mathcal{L}}} \sum_{i,\sigma} (c_{i,\sigma}^\dagger d_\sigma + d_\sigma^\dagger c_{i,\sigma}) \\ &= \epsilon \hat{n} + U \hat{n}_\uparrow \hat{n}_\downarrow + v \sum_{i,\sigma} (f_\sigma^\dagger d_\sigma + d_\sigma^\dagger f_\sigma), \end{aligned} \quad (3)$$

where we have defined the bath orbital  $f$  through

$$f_\sigma = \frac{1}{\sqrt{\mathcal{L}}} \sum_{i=1}^{\mathcal{L}} c_{i,\sigma}. \quad (4)$$

The QD filling is controlled through the occupancy parameter  $\nu$  defined via

$$\epsilon = U(1/2 - \nu).$$

The particle-hole symmetric point of the QD corresponds to  $\epsilon = -U/2$ , i.e.,  $\nu = 1$ . The hybridization is quantified using  $\Gamma = \pi \rho v^2$  with the density of states

$$\rho = 1/2D = 1/d\mathcal{L}.$$

We use the DMRG to find the ground state and a few lowest excited states in symmetry sectors with conserved particle number  $n$  and z-component of spin  $s_z$ . In these numerical calculations we typically choose  $n$  close to half filling with  $s_z = 0$  for even  $n$  and  $s_z = 1/2$  for odd  $n$ . The method is, however, applicable for any filling, including the dilute limit with low occupancy. We also note at this point that we will be using the terms BCS and BEC mostly as labels for weak-coupling and strong-coupling limits of the Richardson model of a superconductor, and that in this work we are focusing on the impurity effects rather than the physics of the clean superconductor itself; the latter has been reviewed in a number of works [24,43,44,46,58].

The Hamiltonian is written in MPO form with  $9 \times 9$  matrices [50]. The DMRG results are obtained with system size  $\mathcal{L} = 100$ , with maximal MPS matrix dimension of 2000 and the energy convergence criterion set at  $\delta = 10^{-8}$ . System sizes up to  $\mathcal{L} = 2000$  with  $\delta = 10^{-12}$  are realistically achievable, but increasing the system size produces marginal gains. Using  $\mathcal{L} \gtrsim 30$  already gives good results at much smaller computational expense. We set the pairing strength  $\alpha = 0.4$  to ensure that an appropriate amount of energy levels participate in pairing even when they span the entire energy range  $[-1 : 1]$ .

The SC-QD models can also be reliably solved by the numerical renormalization group [38,59–67] as well as with continuous-time Quantum Monte Carlo (QMC) using  $U$  [68] and hybridization [69–72] expansion. These methods require a weakly interacting bath and are thus limited to the mean-field BCS description of superconductivity. The RM without the impurity has been treated by QMC in the canonical ensemble [73], and its strong coupling limit has been investigated by expanding the Richardson's solution in powers of  $1/\alpha$  using pseudospin operators [74]. Our DMRG approach is currently the only reliable technique to address the full interacting problem in all parameter regimes.

In the flat-band limit ( $\gamma = 0$ , i.e.,  $D = 0$  or  $\epsilon_i \equiv 0$ ), two renormalization processes associated with the kinetic energy of band electrons no longer occur. These are the renormalization of the exchange interaction from the bare Kondo exchange coupling  $J_K = 8\Gamma/\pi\rho U$  to the scale of the exponentially lower Kondo temperature  $T_K = \exp(-1/\rho J_K)$ , and the renormalization of the pairing interaction from the bare scale of attractive coupling  $g$  to the scale of the exponentially lower SC gap  $\Delta = \exp(-1/\rho g)$ . Both renormalization processes have exactly the same origin: the kinetic energy (dispersion) of the conduction band electrons.

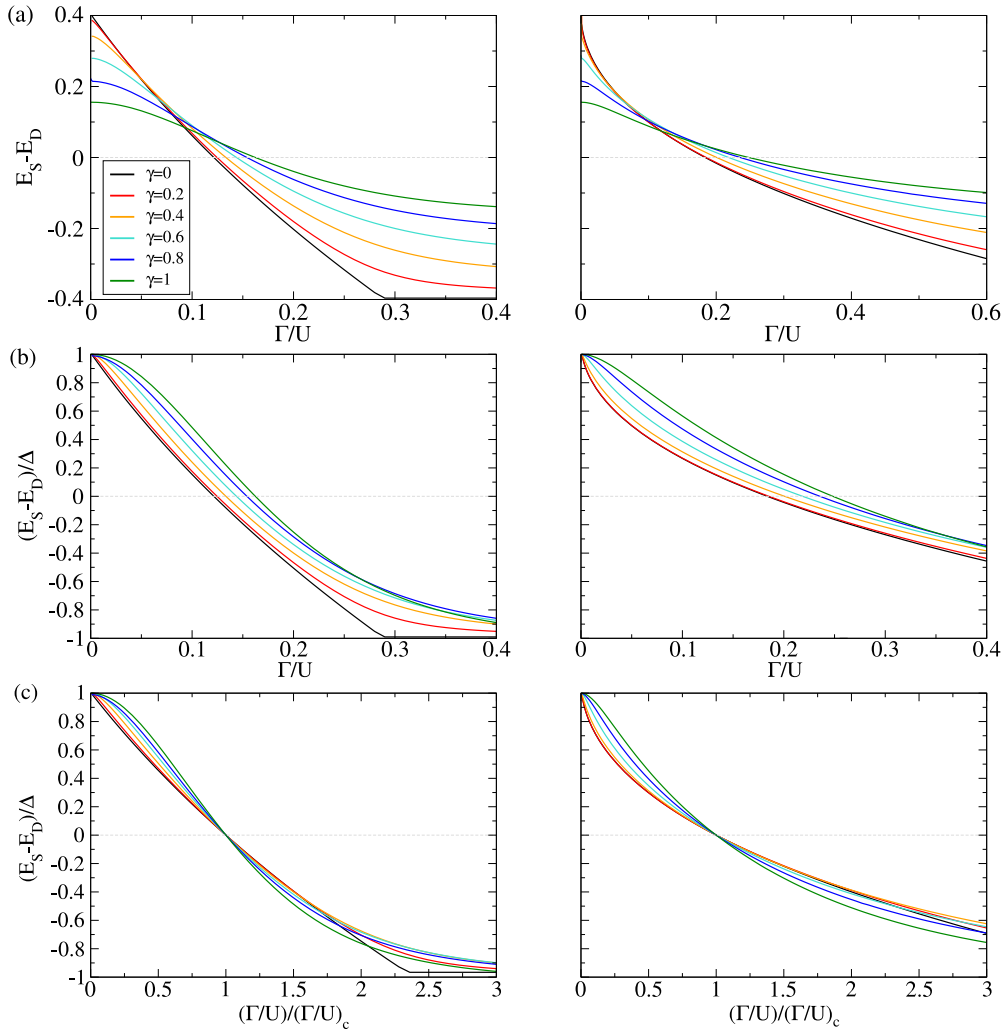


FIG. 1. Singlet-doublet energy difference  $E_{\text{YSR}} = E_S - E_D$  as a function of the hybridization  $\Gamma$  for a range of bandwidths  $\gamma$ . Energy difference  $E_S - E_D$  is expressed either in (a) absolute units or (b), (c) rescaled by the SC gap  $\Delta$ . In panel (c), the horizontal axis is furthermore rescaled so that the singlet-doublet transition points coincide. The parameters are  $\alpha = 0.4$ , strong electron repulsion  $U/\Delta_0 = 40$  (left column) and moderate repulsion  $U/\Delta_0 = 5$  (right column), where  $\Delta_0 \approx 0.16$  is the gap at  $\gamma = 1$ , and particle-hole symmetric tuning  $\nu = 1$ . The results have been corrected for the finite-size effects as described in Ref. [50].

### III. NUMERICAL RESULTS FOR THE BCS-BEC CROSS-OVER

The flattening of the band (and the BCS-BEC crossover) correspond to a variation of the bandwidth rescaling parameter from  $\gamma = 1$  to  $\gamma = 0$ . In this section we present the evolution of the subgap spectra in this crossover.

#### A. Excitation energies

Figure 1 shows the excitation energy of the subgap state at the particle-hole symmetric point ( $\epsilon = -U/2$ ) as a function of the hybridization strength  $\Gamma$ . Increasing  $\Gamma$  strengthens the exchange coupling  $J_K$  between the impurity spin and the quasiparticles:  $J_K = 8\Gamma/\pi U\rho$  [75]. This leads to the formation of the subgap singlet (Yu-Shiba-Rusinov) bound state which detaches from the edge of the continuum of Bogoliubov states [33,35,59,62,76]. As  $\Gamma$  is increased, the subgap descends deeper in the gap and eventually becomes the new ground state of the system; this is known as the doublet-singlet

quantum phase transition and occurs when the characteristic scale of spin-flip processes (Kondo temperature) becomes of the same order as the superconducting gap [32,33,59,60,63]. We consider two cases,  $U/\Delta_0 = 40$  and  $U/\Delta_0 = 5$ , where  $\Delta_0$  is the SC gap in the  $\gamma = 1$  limit. The first case is representative of the large- $U$  limit where the impurity is a pure exchange scatterer (Kondo limit) and the subgap states are well-defined YSR states, while the second is a generic situation where the singlet subgap states have a mixed character due to a stronger proximity effect which admixes states of zero and double impurity occupancy. The first row in Fig. 1 shows the results without any rescaling. With  $\Gamma$  increasing from zero, we see the YSR singlet state detach from the continuum of Bogoliubov states and cross the zero energy-difference line at  $\Gamma = \Gamma_c$  at which point it becomes the ground state of the system. We thus reproduce the well-known results for the qualitative evolution of the subgap states as a function of  $\Gamma$  for all bandwidths  $\gamma$  of the superconductor. It may be remarked that on one side of the cross-over the quantum phase transition is controlled by

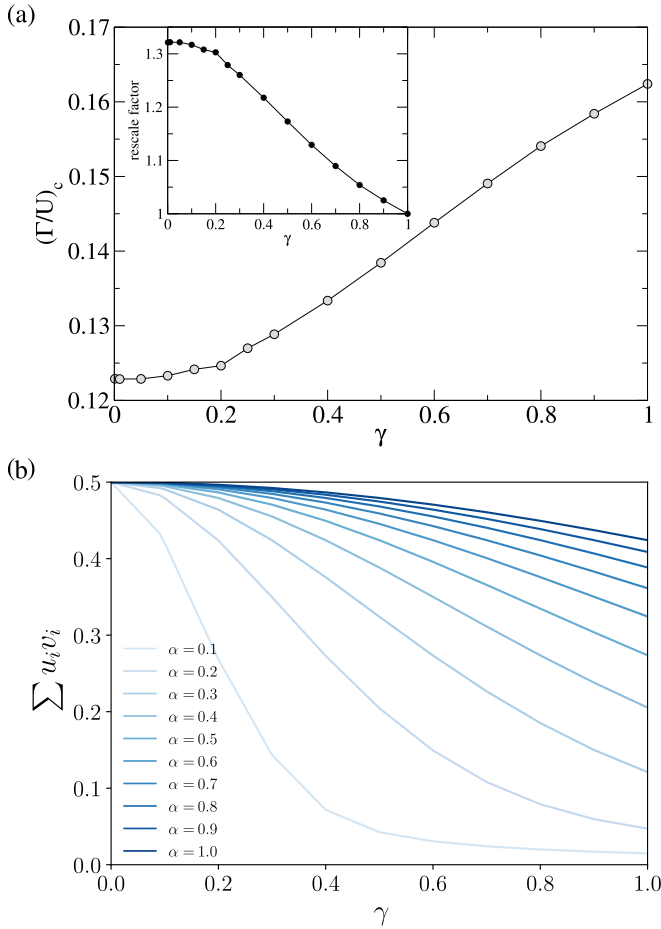


FIG. 2. (a) Bandwidth  $\gamma$  dependence of the transition point  $(\Gamma/U)_c$ . The inset shows the rescaling factor for the hybridization strength that would be required to obtain equivalent results. (b) Pairing strength  $\bar{\Delta}$  dependence on  $\gamma$ . It measures the proportion of levels which contribute in pairing, with all levels contributing equally when  $\bar{\Delta} = 1/2$ .

the ratio of renormalized quantities  $T_K/\Delta$ , while on the other side it is controlled by the ratio of unrenormalized parameters  $J_K/g$ .

To make a more definite statement on the quantitative effects of varying bandwidth  $\gamma$ , we now rescale the results in two steps: (1) we rescale the energies in terms of the SC gap at given  $\gamma$  (second row), (2) we furthermore rescale the  $\Gamma/U$  axis so that the singlet-doublet transition points for all  $\gamma$  coincide (third row). These fully rescaled results demonstrate a reasonably good overlap, showing that during the BCS to BEC crossover the changes in the YSR excitation energy are only quantitative and actually rather small. This is one of the key results of this work.

Figure 2(a) presents the transition point  $(\Gamma/U)_c$  extracted from Fig. 1. The hybridization rescaling factor used in the bottom row of Fig. 1 is shown in the inset. By decreasing the bandwidth  $\gamma$  we allow more levels to participate in hopping processes resulting in larger effect of hybridization  $\Gamma$ . The transition point thus moves to smaller value of  $\Gamma$  with decreasing bandwidth  $\gamma$ . It should be, however, noted that the

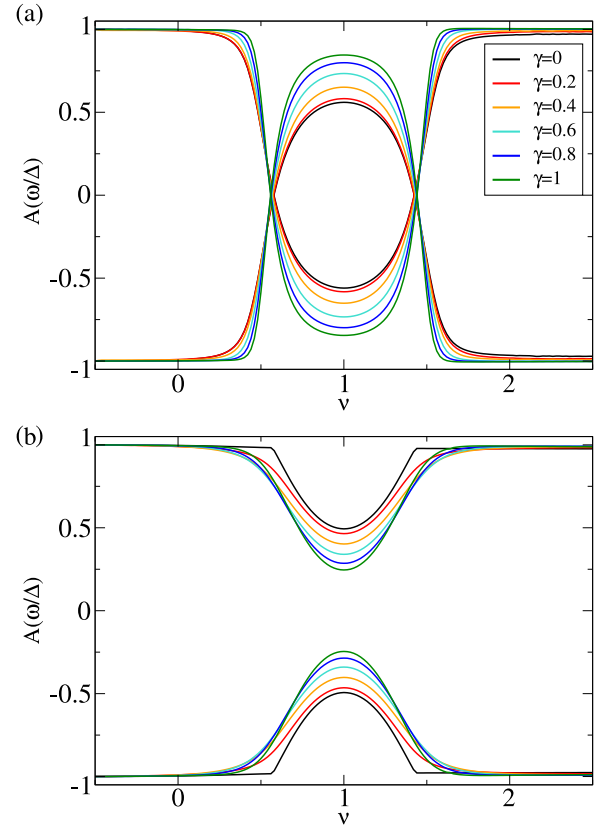


FIG. 3. Gate-voltage dispersion of the subgap states for two values of hybridization: (a)  $\Gamma/U = 0.05$ , (b)  $\Gamma/U = 0.2$ . Other parameters are  $\alpha = 0.4$ ,  $U/\Delta_0 = 40$ . The frequencies are rescaled by  $\Delta$ .

change is rather modest, by approximately 30% for the chosen parameter set.

To better understand the effects of the bandwidth reduction, we plot in Fig. 2(b) the  $\gamma$  dependence of the pairing correlations  $\sum_i u_i v_i$ , where  $u_i = \langle c_{i\downarrow} c_{i\uparrow} c_{i\uparrow}^\dagger c_{i\downarrow}^\dagger \rangle^{1/2}$  and  $v_i = \langle c_{i\uparrow}^\dagger c_{i\downarrow}^\dagger c_{i\downarrow} c_{i\uparrow} \rangle^{1/2}$ , for a range of pairing interaction strengths  $\alpha$ . This sum measures the proportion of levels that contribute to pairing, with all levels contributing equally in the limiting case of saturated sum  $\sum_i u_i v_i = 1/2$ . Similarly as observed in Fig. 2(a), the decrease in bandwidth allows more levels to contribute in pairing processes, strengthening the correlations. Increasing the pairing strength  $\alpha$  at given bandwidth results in qualitatively the same crossover as decreasing the bandwidth  $\gamma$ , illustrating the two possible ways of probing the crossover between the weak-coupling and strong-coupling (BEC-BCS) regimes. The pairing correlations in the zero bandwidth limit, where all curves converge to the saturated value for the half-filled band, are further discussed in Sec. IV A 1.

The subgap states in QDs coupled to SCs can also be tuned by the gate voltage that shifts the impurity energy level  $\epsilon$ . The further away from the half-filled special point ( $\nu = 1$ ) the QD is tuned, the less magnetic it behaves: far from  $\nu = 1$  the subgap state is expected to merge back with the continuum. In Fig. 3 we show the gate-voltage dispersion for two fixed values of  $\Gamma/U$ , on either side of the singlet-doublet transition value  $\Gamma_c$  at  $\nu = 1$ , so that in one case we find the typical



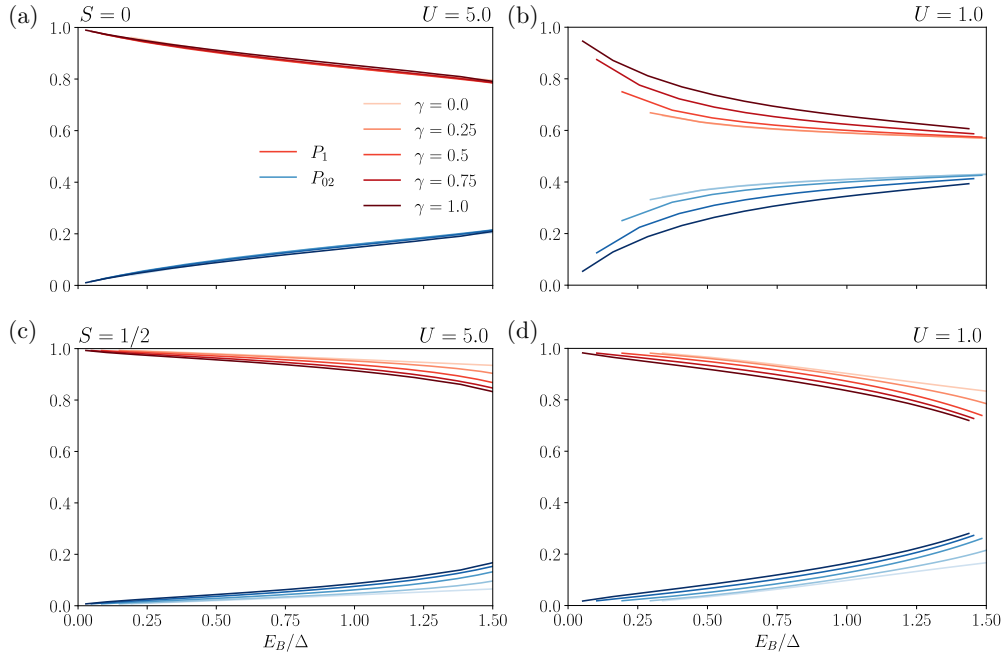


FIG. 4. Impurity occupation probabilities  $P_1$  and  $P_{02}$  versus binding energy  $E_B = E_S - (E_D + \Delta)$  for different values of bandwidth  $\gamma$  for the singlet (top) and doublet (bottom) ground state.  $E_B$  is the energy gain of the subgap singlet state compared to the first excited (decoupled) singlet state and is rescaled by the optical gap  $\Delta$  for each  $\gamma$ . The pairing interaction strength is  $\alpha = 0.4$ .

YSR ring (eye-shaped dispersion) and in the other Gaussian shaped curves. We again observe that we may reproduce the well-known results for the evolution of the subgap states as a function of  $\epsilon$  for all bandwidths  $\gamma$  of the superconductor. On quantitative level, after scaling the energies by the gap as in the present plot, we find a good overlap which could be further improved by adjusting the  $\Gamma$  values as described above.

### B. Subgap state properties

In addition to the approximate overlap of the YSR state energies, we also find a high degree of similarity in the state properties across the crossover. As an example, in Fig. 4 we plot the probabilities that the impurity level is singly occupied ( $P_1$ ) or doubly occupied/empty ( $P_{02}$ ) versus binding energy  $E_B = E_S - (E_D + \Delta)$ . These are obtained from the reduced density matrix for the impurity site and contain important information about the nature of the states.

In the top row we plot the singlet ground state. For the singlet YSR state we expect  $P_\uparrow = P_\downarrow = 1/2$  and thus  $P_1 = 1$ . With increasing  $E_B$  (by increasing the hybridization  $\Gamma$ ) the local magnetic moment of the impurity level decreases due to larger charge fluctuations.  $P_{02}$  measures the contribution of the proximitized ABS state, which becomes dominant in the limit of large  $\Gamma/U$ . Figure 4(a) shows that this behavior persists throughout the BCS-BEC transition. In this case with  $U \gg \Delta$  we find good overlap of the curves. The situation away from this limit, where  $U \approx \Delta$ , is shown in Fig. 4(b). Here the magnitude of charge fluctuations depend not only on  $\Gamma/U$  but also on  $\Gamma/\Delta$ . The fact that two different scales control the charge fluctuations decreases the quality of the collapse, but the qualitative agreement for different  $\gamma$  remains.

The bottom row shows the doublet ground state, where the mechanism of changing state character is a bit different.

Increasing  $E_B$  increases the admixture of the excited doublet state, which is identical to the YSR singlet with an additional free quasiparticle in the bath. This excited state transforms from a YSR-like singlet to an ABS-like proximitized state (as discussed in the previous paragraph), resulting in the decrease of  $P_1$ , which is, however, more gradual compared to the singlets. This is most obvious when comparing the two cases with smaller  $U$  in Figs. 4(b) and 4(d).

We note that we find a similar qualitative agreement for different  $\gamma$  for many state properties. This is an important result in its own, as it implies that it is possible to use the flat-band solutions to investigate the nature of the low energy states in realistic QD-SC systems.

## IV. EXACT SOLUTION FOR THE FLAT-BAND LIMIT

In the following we show that the flat-band limit is analytically solvable even in the presence of a magnetic impurity, in the sense of being reducible to numerical diagonalizations of very small matrices. This model provides a conceptually clear picture of all phenomena occurring in ultrasmall SCs coupled to quantum dots and provides exact benchmark results for testing other approaches. The method works for arbitrary parameter values and can be applied for any band filling, from the dilute limit to half filling.

### A. Eigenstates of the superconductor

We take the  $\epsilon_i \equiv 0$  limit of the RM (also known as the “seniority model” in the context of nuclear physics [77]) and write the SC part of the Hamiltonian as

$$H = -\frac{g}{\mathcal{L}} \sum_{i,j} c_{i\uparrow}^\dagger c_{i\downarrow}^\dagger c_{j\downarrow} c_{j\uparrow} = -\frac{g}{\mathcal{L}} \sum_{i,j} A_i^\dagger A_j, \quad (5)$$

where  $A_j = c_{j\downarrow}c_{j\uparrow}$  are the hard-core boson operators with the commutation rule:

$$[A_i, A_j^\dagger] = \delta_{ij}(1 - \hat{n}_i), \quad (6)$$

where  $\hat{n}_i = \sum_{\sigma} c_{i\sigma}^\dagger c_{i\sigma}$  is the level occupancy operator. The following relations also hold:

$$\begin{aligned} A_i^2 &\equiv 0, \\ (A_i^\dagger)^2 &\equiv 0, \\ A_i^\dagger A_i &= \hat{P}_{2,i} = \hat{n}_{i\uparrow}\hat{n}_{i\downarrow}, \\ A_i A_i^\dagger &= \hat{P}_{0,i} = 1 - \hat{n}_i + \hat{n}_{i\uparrow}\hat{n}_{i\downarrow}. \end{aligned} \quad (7)$$

The operators  $\hat{P}_{0,i}$  and  $\hat{P}_{2,i}$  are the projectors on the subspace with occupancy 0 or 2 on level  $i$ .

The seniority model can be diagonalized making use of its SU(2) symmetry [77–79]. Here we will construct the eigenstates by exponentiating the creation operator for electron pairs and obtain eigenvalues directly by algebraic means.

The Hamiltonian  $H$  is not particle-hole (p-h) symmetric. The symmetry can be restored by adding a potential energy term:

$$\tilde{H} = H + \tilde{\epsilon} \sum_i \hat{n}_i, \quad (8)$$

with

$$\tilde{\epsilon} = \frac{g}{2\mathcal{L}} = \frac{\alpha d}{2} = \frac{\alpha}{\mathcal{L}},$$

using  $D \equiv 1$  as energy unit.

Let  $\mathcal{U}$  be the set of “unblocked levels” (those occupied by either 0 or 2 electrons). The blocked levels  $\mathcal{B}$  (those with occupancy 1) do not participate in pairing and they fully decouple from the problem in the absence of an impurity, thus in this subsection all the sums that follow are constrained to the set of unblocked levels. We will also use the same symbol  $\mathcal{U}$  to denote the number of unblocked levels, since this leads to no ambiguity. In the absence of quasiparticles no level is blocked,  $\mathcal{B} = \emptyset$ , and we have  $\mathcal{U} = \mathcal{L}$ .

We introduce the equal-weight linear combination of hard-core operators corresponding to all unblocked levels,

$$B = \frac{1}{\sqrt{\mathcal{U}}} \sum_i^{\mathcal{U}} A_i, \quad (9)$$

so that

$$H = -g \frac{\mathcal{U}}{\mathcal{L}} B^\dagger B + H_{\text{blocked}}. \quad (10)$$

Dropping the blocked subspace from this point on, the full Hamiltonian including the p-h symmetry restoring energy shift is thus

$$\tilde{H} = -g \frac{\mathcal{U}}{\mathcal{L}} B^\dagger B + \frac{\alpha}{\mathcal{L}} \hat{N}, \quad (11)$$

where

$$\hat{N} = \sum_i^{\mathcal{U}} \hat{n}_i \quad (12)$$

is the total number of electrons in the *unblocked* subset of levels (i.e., the energy of unpaired electrons in the blocked levels is not included).

The eigenstates for  $M$  Cooper pairs in the  $\mathcal{U}$  levels are

$$\Psi_M^{\mathcal{L},\mathcal{U}} = \mathcal{N}_M |M\rangle = \mathcal{N}_M (B^\dagger)^M |0\rangle, \quad (13)$$

where  $|M\rangle = (B^\dagger)^M |0\rangle$  and  $\mathcal{N}_M$  is a normalization factor (see Appendix B). In the following, the superscripts  $\mathcal{L}, \mathcal{U}$  in  $\Psi_M^{\mathcal{L},\mathcal{U}}$  will be dropped when no ambiguity may result; when a single superscript is indicated, it corresponds to  $\mathcal{U}$ .

We have  $H\Psi_0 = 0$  and  $H\Psi_1 = -g(\mathcal{U}/\mathcal{L})\Psi_1$ . General eigenvalues can be computed by recursion (see Appendix A), finding

$$H|M\rangle = -g(\mathcal{U}/\mathcal{L})c_M|M\rangle, \quad (14)$$

with

$$c_M = \frac{(1 + \mathcal{U} - M)M}{\mathcal{U}}. \quad (15)$$

The ground-state energy of a system of size  $\mathcal{L}$  with  $\mathcal{U}$  unblocked levels containing  $M$  Cooper pairs is thus

$$E_M^{\mathcal{L},\mathcal{U}} = -2\alpha \frac{(1 + \mathcal{U} - M)M}{\mathcal{L}}, \quad (16)$$

while the shifted eigenvalues (corresponding to  $\tilde{H}$ ) are

$$\tilde{E}_M^{\mathcal{L},\mathcal{U}} = -2\alpha \frac{(\mathcal{U} - M)M}{\mathcal{L}}. \quad (17)$$

The interpretation of this expression is very simple. Each of the  $M$  Cooper pairs resonates with the  $\mathcal{U} - M$  empty levels in the system, each combination contributing  $2\alpha/\mathcal{L} = G$  to the total energy. We note that  $\tilde{E}$  does not include the energy of single electrons in the blocked levels, which is not included in Eq. (11). We therefore define the total energy  $\hat{E}$  as

$$\begin{aligned} \hat{E}_M^{\mathcal{L},\mathcal{U}} &= \tilde{E}_M^{\mathcal{L},\mathcal{U}} + \frac{\alpha}{\mathcal{L}}(\mathcal{L} - \mathcal{U}) \\ &= \alpha \frac{-2(\mathcal{U} - M)M + \mathcal{L} - \mathcal{U}}{\mathcal{L}}. \end{aligned}$$

For half filling,  $n = \mathcal{L}$  and  $M = \mathcal{L}/2$ , and one has for  $\mathcal{U} = \mathcal{L}$

$$\tilde{E}_{\mathcal{L}/2}^{\mathcal{L},\mathcal{L}} = -\alpha \frac{\mathcal{L}}{2} \equiv \mathcal{E}. \quad (18)$$

Also, we find

$$\tilde{E}_{\mathcal{L}/2+1}^{\mathcal{L},\mathcal{L}} = \mathcal{E} + \frac{2\alpha}{\mathcal{L}}, \quad \tilde{E}_{\mathcal{L}/2+2}^{\mathcal{L},\mathcal{L}} = \mathcal{E} + \frac{8\alpha}{\mathcal{L}}, \dots, \quad (19)$$

thus additional Cooper pairs have an energy cost of order  $1/\mathcal{L}$ . In the thermodynamic limit ( $\mathcal{L} \rightarrow \infty$ ), the ground state would be macroscopically degenerate, as is the case in bulk SCs.

We now consider a single quasiparticle in the system, i.e., we make one of the  $\mathcal{L}$  levels singly occupied, so that  $\mathcal{U} = \mathcal{L} - 1$ . The energy cost in the  $n = \mathcal{L} + 1$  charge sector is

$$E^{qp,+} = (\tilde{E}_{\mathcal{L}/2}^{\mathcal{L},\mathcal{L}-1} + \tilde{\epsilon}) - \mathcal{E} = \left(1 + \frac{1}{\mathcal{L}}\right)\alpha. \quad (20)$$

and in the  $n = \mathcal{L} - 1$  charge sector it is

$$E^{qp,-} = (\tilde{E}_{\mathcal{L}/2-1}^{\mathcal{L},\mathcal{L}-1} + \tilde{\epsilon}) - \mathcal{E} = \left(1 + \frac{1}{\mathcal{L}}\right)\alpha. \quad (21)$$

In the equal-charge ( $n = \mathcal{L}$ ) sector, the lowest excitation contains two quasiparticles. Its energy is

$$(\tilde{E}_{\mathcal{L}/2-1}^{\mathcal{L},\mathcal{L}-2} + 2\tilde{\epsilon}) - \mathcal{E} = 2\alpha. \quad (22)$$

The cost of a quasiparticle excitation in flat-band superconductors is equal to the bare pairing interaction [10,80,81].

### 1. Pairing strength

The strength of pairing correlations may be quantified by evaluating the following correlators [58]:

$$\begin{aligned} \bar{v}_i &= \langle c_{i\uparrow}^\dagger c_{i\downarrow}^\dagger c_{i\downarrow} c_{i\uparrow} \rangle^{1/2} = \langle A_i^\dagger A_i \rangle^{1/2}, \\ \bar{u}_i &= \langle c_{i\downarrow} c_{i\uparrow} c_{i\uparrow}^\dagger c_{i\downarrow}^\dagger \rangle^{1/2} = \langle A_i A_i^\dagger \rangle^{1/2}, \\ \bar{\Delta} &= \frac{g}{\mathcal{L}} \sum_i \bar{v}_i \bar{u}_i, \\ \bar{\Delta}' &= \frac{g}{\mathcal{L}} \sum_i (\langle n_{i\uparrow} n_{i\downarrow} \rangle - \langle n_{i\uparrow} \rangle \langle n_{i\downarrow} \rangle)^{1/2}. \end{aligned} \quad (23)$$

$\bar{v}_i$  is the amplitude to find a pair of states occupied, while  $\bar{u}_i$  is the amplitude to find a pair of states empty. If the system is homogeneous, then all amplitudes are the same,  $\bar{v} \equiv \bar{v}_i$  and  $\bar{u} \equiv \bar{u}_i$ , so that

$$\bar{\Delta} = g\bar{v}\bar{u}. \quad (24)$$

Both  $\bar{\Delta}$  and  $\bar{\Delta}'$  reduce to  $\Delta_{\text{BCS}}$  in the thermodynamic limit [43].

At half filling, the results is obviously  $\bar{v}^2 = \bar{u}^2 = 1/2$ , because there is probability 1/2 to find any given level unoccupied and the same probability to find it doubly occupied, and by construction it cannot be singly occupied, since no level is blocked. Thus,

$$\bar{\Delta} = \frac{g}{2} = \alpha. \quad (25)$$

In general, the amplitudes  $\bar{v}_i$  and  $\bar{u}_i$  are related, since  $A_i^\dagger A_i = A_i^\dagger A_i - (1 - \hat{n}_i)$ , thus

$$\bar{v}^2 = \bar{u}^2 - \langle \Psi_M | (1 - \hat{n}_i) | \Psi_M \rangle = \bar{u}^2 - 1 + \frac{2M}{\mathcal{U}}. \quad (26)$$

In the subspace where all levels are either unoccupied or doubly occupied, we also have  $\bar{v}^2 + \bar{u}^2 = 1$ . Then it follows immediately that

$$\bar{v}^2 = \frac{M}{\mathcal{U}}, \quad \bar{u}^2 = \frac{\mathcal{U} - M}{\mathcal{U}}, \quad \bar{\Delta} = 2\alpha \frac{\sqrt{M(\mathcal{U} - M)}}{\mathcal{U}}. \quad (27)$$

The other estimate,  $\bar{\Delta}'$ , can also be easily computed:

$$\bar{\Delta}' = \frac{g}{\mathcal{L}} \mathcal{U} \left( \frac{M}{\mathcal{U}} - \frac{M}{\mathcal{U}} \frac{M}{\mathcal{U}} \right)^{1/2}, \quad (28)$$

because in a homogeneous system  $\langle \hat{n}_{i\uparrow} \hat{n}_{i\downarrow} \rangle = \langle \hat{P}_{2i} \rangle = M/\mathcal{U}$  and  $\langle n_{i\sigma} \rangle = M/\mathcal{U}$ . At half filling, this yields

$$\bar{\Delta}' = \alpha.$$

In this flat-band model, the pairing correlations are thus directly proportional to the coupling-strength  $\alpha$ . This is a known feature of strong-coupling SC systems [10,80,81]. The exponential reduction in the standard weak-coupling BCS theory is a consequence of the finite width of the electron band.

### B. YSR states for a Kondo impurity

We now include a magnetic impurity into consideration. First we consider the case of a pure exchange scatterer and take the large- $U$  limit of the impurity Hamiltonian at  $\nu = 1$  to obtain an effective Kondo Hamiltonian [75,82]:

$$H_{\text{QD}} = \frac{J}{\mathcal{L}} \sum_{i,j} \mathbf{S} \cdot \mathbf{s}_{i,j}, \quad (29)$$

where the Kondo exchange coupling is

$$J = 8v^2/U = \frac{16}{\pi} (\Gamma/U), \quad (30)$$

and the interlevel spin operators are defined as

$$\mathbf{s}_{i,j} = \frac{1}{2} c_{i,\alpha}^\dagger \boldsymbol{\sigma}_{\alpha,\beta} c_{j,\beta}. \quad (31)$$

Here  $\boldsymbol{\sigma} = \{\sigma^x, \sigma^y, \sigma^z\}$  is a vector of Pauli matrices and the expression is summed over repeated spin indexes  $\alpha$  and  $\beta$ . Note that in this discrete model  $\Gamma$  does not have the significance of a level width, but it nevertheless quantifies the coupling strength. Equivalently, we may write

$$H_{\text{QD}} = J\mathbf{S} \cdot \mathbf{s}, \quad (32)$$

with  $\mathbf{s}$  the spin of an electron in the orbital  $f$ , see Eq. (4),

$$\mathbf{s} = \frac{1}{2} f_\alpha^\dagger \boldsymbol{\sigma}_{\alpha,\beta} f_\beta. \quad (33)$$

For half filling with  $M = \mathcal{L}/2$  Cooper pairs (assuming even  $\mathcal{L}$ ) and one electron in the impurity level (odd total number of electrons  $n = \mathcal{L} + 1$ , i.e., spin-doublet sector), the impurity remains entirely decoupled from the SC in the ground state. The reason is that the product state  $\psi = |M\rangle \otimes |\sigma\rangle$  is an eigenstate of  $H_{\text{QD}}$ . First we note that the state  $|M\rangle$  is an eigenstate of  $\hat{s}_z$  with  $\hat{s}_z |M\rangle = 0$ . We thus only need to consider the transverse  $S^- S^+$  terms. This operator is composed of pairs

$$c_{i\uparrow}^\dagger c_{j\downarrow} + c_{j\uparrow}^\dagger c_{i\downarrow}. \quad (34)$$

We have

$$[c_{i\uparrow}^\dagger c_{j\downarrow}, A_j^\dagger] = -c_{i\uparrow}^\dagger c_{j\uparrow}^\dagger, \quad [c_{j\uparrow}^\dagger c_{i\downarrow}, A_i^\dagger] = c_{i\uparrow}^\dagger c_{j\uparrow}^\dagger. \quad (35)$$

This leads to a cancellation for any  $i \neq j$  pair. Furthermore, the diagonal  $i = j$  terms are trivially zero due to Pauli exclusion principle. Thus, we have  $S^+ |M\rangle = 0$ , showing that  $|M\rangle$  is indeed an eigenstate.

The same commutation relations also establish that the pure exchange interaction preserves the decoupling between the blocked (singly occupied) levels  $\mathcal{B}$  and the unblocked (zero or double occupancy) levels  $\mathcal{U}$ . Thus, the Hamiltonian in the subspace of  $\mathcal{B}$  blocked levels is

$$H_{\mathcal{B}} = J\mathbf{S} \cdot \mathbf{s}, \quad (36)$$

where  $\mathbf{s}$  is now constrained only over the blocked levels. This is an exact statement. The ground state in the even occupancy  $n = \mathcal{L} + 2$  sector results from the interaction between the single quasiparticle and the impurity spin (i.e., the YSR singlet state). This is clearly a simple two-body problem of two spins coupled by an isotropic exchange interaction, with one singlet eigenstate at energy  $-3/4J$  and one triplet eigenstate at energy  $+1/4J$ . The creation of the quasiparticle has an energy

cost of  $(1 + 1/\mathcal{L})\alpha$ . The excitation energy is thus

$$E_{\text{YSR}} = \left(1 + \frac{1}{\mathcal{L}}\right)\alpha - \frac{3J}{4}. \quad (37)$$

The YSR singlet binding energy is

$$\Delta E = E^{qp,+} - E_{\text{YSR}} = \frac{3}{4}J = \frac{12}{\pi}(\Gamma/U). \quad (38)$$

There is a YSR triplet state in the ‘‘continuum’’ with an energy surplus of  $1/4J$ .

### C. YSR states for an Anderson impurity

At finite  $U$ , an electron from a doubly occupied bath level can hop on the impurity site, and an electron can hop from the impurity site to an unoccupied bath level. The decoupling between the blocked levels  $\mathcal{B}$  and the unblocked levels  $\mathcal{U}$  is lost: the subsectors mix. We need to separately discuss the cases with different fermionic parity (and consequently total spin).

#### 1. Odd total number of electrons (spin-doublet)

We first consider the case with an odd total number of electrons. The  $z$  component of total spin is a conserved quantity; we will work in the  $s_z = 1/2$  subspace. The following normalized states are coupled by the hopping term:

$$\begin{aligned} \psi_{0,b} &= |0\rangle \otimes c_{b\uparrow}^\dagger \Psi_M^{\mathcal{L}\setminus b}, \\ \Psi_1 &= |1\rangle \otimes \Psi_M^{\mathcal{L}}, \\ \psi_{1,bb'} &= |1\rangle \otimes c_{b\uparrow}^\dagger c_{b'\downarrow}^\dagger \Psi_{M-1}^{\mathcal{L}\setminus b,b'}, \\ \psi_{2,b} &= |2\rangle \otimes c_{b\uparrow}^\dagger \Psi_{M-1}^{\mathcal{L}\setminus b}. \end{aligned} \quad (39)$$

The ket  $|i\rangle$  represents the impurity state with  $i$  electrons, defined as  $|1\rangle = d_\uparrow^\dagger|0\rangle$  and  $|2\rangle = d_\uparrow^\dagger d_\downarrow^\dagger|1\rangle$ . In  $\psi_{0,b}$  and  $\psi_{2,b}$  the level  $b$  is blocked; here  $1 \leq b \leq \mathcal{L}$ . The notation  $\mathcal{L}\setminus b$  in the superscript denotes that the set of unblocked levels  $\mathcal{U}$  encompasses all levels except  $b$ , while the subscripts represent the number of Cooper pairs. In a similar vein, in  $\psi_{1,bb'}$  two levels are blocked. We note that states with two quasiparticles with equal spin in the superconductor (and opposite spin in the QD, such that the total spin is  $S = 1/2$  and  $S_z = 1/2$ ) do not couple with the subset of states in Eq. (39) in the flat-band limit.

We now form normalized equal-weight superpositions of  $\psi_{0,b}$  and  $\psi_{2,b}$ ,

$$\Psi_0 = \frac{1}{\sqrt{\mathcal{L}}} \sum_{b=1}^{\mathcal{L}} \psi_{0,b}, \quad \Psi_2 = \frac{1}{\sqrt{\mathcal{L}}} \sum_{b=1}^{\mathcal{L}} \psi_{2,b},$$

as well as

$$\Psi'_1 = \frac{1}{\sqrt{\mathcal{L}(\mathcal{L}-1)}} \sum_{b \neq b'} \psi_{1,bb'}.$$

Note that the double sum is over all  $\mathcal{L}$  so the two quasiparticles form a singlet state. For large  $\mathcal{L}$  this simplifies to

$$\Psi'_1 \approx \frac{1}{\mathcal{L}} \sum_{b \neq b'} \psi_{1,bb'}.$$

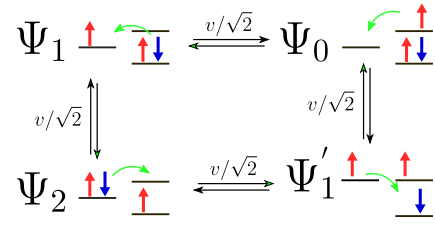


FIG. 5. Schematic representation of the states coupled in the doublet subspace. In the flat-band limit, no other states couple with this subset. Left line: QD level. Right lines: SC levels. Quasiparticles (singly occupied SC levels) represent superpositions of states where the single electron occupies any of the superconductor  $\mathcal{L}$  levels. Green arrows represent the hopping process resulting in the next state (counterclockwise).

The energies of the doublet states  $\Psi$  are

$$\begin{aligned} E_0^D &= \tilde{E}_M^{\mathcal{L},\mathcal{L}-1} + \tilde{\epsilon} - \epsilon, \\ E_1^D &= \tilde{E}_M^{\mathcal{L},\mathcal{L}}, \\ E_1^{D'} &= \tilde{E}_{M-1}^{\mathcal{L},\mathcal{L}-2} + 2\tilde{\epsilon}, \\ E_2^D &= \tilde{E}_{M-1}^{\mathcal{L},\mathcal{L}-1} + \tilde{\epsilon} + \epsilon + U. \end{aligned} \quad (40)$$

Here we included the energy shifts  $\tilde{\epsilon}$  (hence we use energies  $\tilde{E}$ ), which are important for this consideration, and we have subtracted  $\epsilon$ . The superscript  $D$  denotes that these are energies in the spin-doublet subspace.

To compute the matrix elements, we make use of an expression derived in Appendix B after setting  $M = \mathcal{L}/2$ :

$$f_\sigma^\dagger \Psi_{\mathcal{L}/2}^{\mathcal{L}} = \frac{1}{\sqrt{2}} \frac{1}{\sqrt{\mathcal{L}}} \sum_b c_{b,\sigma}^\dagger \Psi_{\mathcal{L}/2}^{\mathcal{L}\setminus b}, \quad (41)$$

thus  $f_\sigma^\dagger d_\sigma \Psi_1 = (1/\sqrt{2})\Psi_0$ . An analogous expression can be obtained for  $f_\sigma \Psi_{\mathcal{L}/2}^{\mathcal{L}}$ , giving  $d_\sigma^\dagger f_\sigma \Psi_1 = (1/\sqrt{2})\Psi_2$ . In a similar way we obtain all other matrix elements.

We obtain a four-level problem with the Hamiltonian in the orthonormal basis  $\{\Psi_1, -\Psi'_1, \Psi_0, \Psi_2\}$  that can be expressed in the large- $\mathcal{L}$  limit and at half-filling as

$$H_{\text{eff}}^D = \begin{pmatrix} E_1^D & 0 & v/\sqrt{2} & -v/\sqrt{2} \\ 0 & E_1^{D'} & v/\sqrt{2} & v/\sqrt{2} \\ v/\sqrt{2} & v/\sqrt{2} & E_0^D & 0 \\ -v/\sqrt{2} & v/\sqrt{2} & 0 & E_2^D \end{pmatrix}. \quad (42)$$

The schematic representation of this Hamiltonian is shown in Fig. 5. The full expression for  $H_{\text{eff}}^D$  for arbitrary  $\mathcal{L}$  and  $M$  with exact matrix elements is given in Appendix D. Close to half filling and for small to moderate  $v$ , the state  $\Psi'_1$  is a highly excited state and plays little role (it admixes in the ground state wavefunction only as a  $v^4$  correction). We may thus drop the second row and second column in the matrix in Eq. (42) and write

$$H_{\text{eff}}^D = \begin{pmatrix} E_1^D & v/\sqrt{2} & -v/\sqrt{2} \\ v/\sqrt{2} & E_0^D & 0 \\ -v/\sqrt{2} & 0 & E_2^D \end{pmatrix}. \quad (43)$$

The eigenenergies can be obtained from the cubic roots. At half filling in the particle-hole symmetric point ( $\epsilon = -U/2$ )



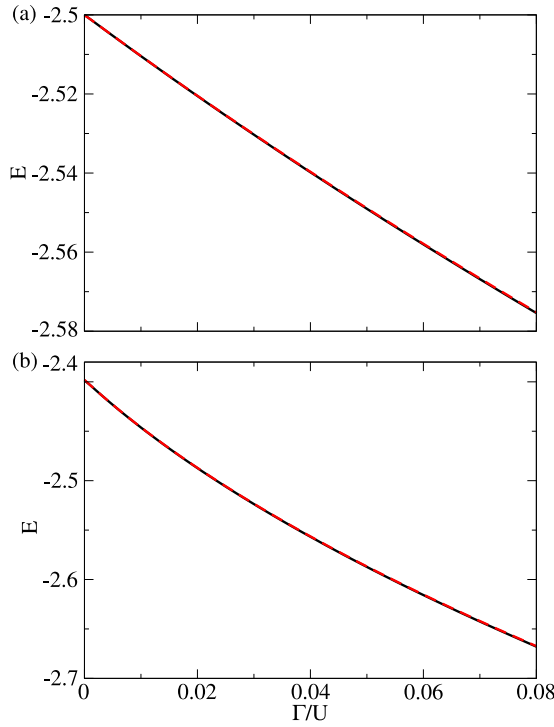


FIG. 6. Ground state eigenenergies in the flat-band limit for  $U = 10\alpha$ , specifically  $\alpha = 0.1$  and  $U = 1$  in units of  $D$ ,  $\mathcal{L} = 50$ . Full line in both panels: DMRG results. (top) Odd-parity (spin-doublet) sector with  $n = \mathcal{L} + 1$ ,  $s_z = 1/2$ . Dashed line: lowest eigenvalue of the Hamiltonian in Eq. (45). (bottom) Even-parity (spin-singlet) sector with  $n = \mathcal{L} + 2$ ,  $s_z = 0$ . Dashed line: lowest eigenvalue of the Hamiltonian in Eq. (55).

the problem simplifies even further. We then have

$$\begin{aligned} E_0^D = E_2^D &= -\alpha \frac{\mathcal{L}}{2} + \alpha + U/2 \equiv E_{02}^D, \\ E_1^D &= -\alpha \frac{\mathcal{L}}{2}. \end{aligned} \quad (44)$$

The eigenvector  $(0,1,1)$  with eigenvalue  $E_{02}^D$  decouples. The ground state can then be obtained by diagonalising the  $2 \times 2$  matrix

$$H_{\text{eff}}^D = \begin{pmatrix} E_1^D & v \\ v & E_{02}^D \end{pmatrix}. \quad (45)$$

Reference calculations demonstrating that the method is exact are presented in Appendix D. Even using the approximate expressions from this section which are strictly correct only in the  $\mathcal{L} \rightarrow \infty$  limit, we find excellent agreement with the DMRG results even at moderate  $\mathcal{L} = 50$ , see Fig. 6 (top panel) where we plot the lowest eigenvalue of  $H_{\text{eff}}^D$  using the dashed line and the reference results as full line.

## 2. Even total number of electrons (spin-singlet)

We now consider the case with an even total number of electrons, specifically  $n = 2M + 2$ , in the spin singlet state. We first enumerate all relevant states in the subspace with  $s_z = 0$ . There are two states with single occupancy of the impurity, while in the sectors with  $n_{\text{imp}} = 0$  and  $n_{\text{imp}} = 2$  we need to include two types of states, those with no quasiparticles and

those with two quasiparticles:

$$\begin{aligned} \Psi_0 &= |0\rangle \otimes \Psi_{M+1}^{\mathcal{L}}, \\ \psi'_{0,bb'} &= |0\rangle \otimes c_{b\uparrow}^\dagger c_{b'\downarrow}^\dagger \Psi_M^{\mathcal{L}\setminus b,b'}, \\ \psi_{1,b,\sigma} &= |\sigma\rangle \otimes c_{b\bar{\sigma}}^\dagger \Psi_M^{\mathcal{L}\setminus b}, \\ \Psi_2 &= |2\rangle \otimes \Psi_M^{\mathcal{L}}, \\ \psi'_{2,bb'} &= |2\rangle \otimes c_{b\uparrow}^\dagger c_{b'\downarrow}^\dagger \Psi_{M-1}^{\mathcal{L}\setminus b,b'}, \end{aligned} \quad (46)$$

with energies

$$\begin{aligned} E_0^S &= \tilde{E}_{M+1}^{\mathcal{L},\mathcal{L}} - \epsilon, \\ E_0^{S'} &= \tilde{E}_M^{\mathcal{L},\mathcal{L}-2} + 2\tilde{\epsilon} - \epsilon, \\ E_1^S &= \tilde{E}_M^{\mathcal{L},\mathcal{L}-1} + \tilde{\epsilon}, \\ E_2^S &= \tilde{E}_M^{\mathcal{L},\mathcal{L}} + \epsilon + U, \\ E_2^{S'} &= \tilde{E}_{M-1}^{\mathcal{L},\mathcal{L}-2} + 2\tilde{\epsilon} + \epsilon + U. \end{aligned} \quad (47)$$

For one electron beyond half filling (i.e., for  $M = \mathcal{L}/2$ ) and  $\epsilon = -U/2$ , this yields

$$\begin{aligned} E_0^S &= -\alpha \frac{\mathcal{L}}{2} + U/2 + \frac{2\alpha}{\mathcal{L}}, \\ E_0^{S'} &= -\alpha \frac{\mathcal{L}}{2} + 2\alpha + U/2 + \frac{2\alpha}{\mathcal{L}} = E_0^S + 2\alpha, \\ E_1^S &= -\alpha \frac{\mathcal{L}}{2} + \alpha + \frac{\alpha}{\mathcal{L}}, \\ E_2^S &= -\alpha \frac{\mathcal{L}}{2} + U/2, \\ E_2^{S'} &= -\alpha \frac{\mathcal{L}}{2} + 2\alpha + U/2 = E_2^S + 2\alpha. \end{aligned} \quad (48)$$

The difference between  $E_0^S$  and  $E_2^S$  is a  $\mathcal{O}(1/\mathcal{L})$  correction,  $E_0^S - E_2^S = 2\alpha/\mathcal{L}$  and vanishes in the thermodynamic limit.

We now form normalized equal superpositions of  $\psi'_{0,bb'}$  and  $\psi'_{2,bb'}$  states:

$$\begin{aligned} \Psi'_0 &= \frac{1}{\sqrt{\mathcal{L}(\mathcal{L}-1)}} \sum_{b \neq b'} \psi'_{0,bb'}, \\ \Psi'_2 &= \frac{1}{\sqrt{\mathcal{L}(\mathcal{L}-1)}} \sum_{b \neq b'} \psi'_{2,bb'}, \end{aligned} \quad (49)$$

we can be simplified in the  $\mathcal{L} \rightarrow \infty$  limit to

$$\begin{aligned} \Psi'_0 &\approx \frac{1}{\mathcal{L}} \sum_{b \neq b'} c_{b\uparrow}^\dagger c_{b'\downarrow}^\dagger \Psi_M^{\mathcal{L}\setminus b,b'}, \\ \Psi'_2 &\approx \frac{1}{\mathcal{L}} \sum_{b \neq b'} c_{b\uparrow}^\dagger c_{b'\downarrow}^\dagger \Psi_{M-1}^{\mathcal{L}\setminus b,b'}. \end{aligned}$$

These are spin-singlet states. Furthermore, we make a normalized spin-singlet combination of  $\psi_{1,b,\sigma}$ :

$$\begin{aligned} \Psi_1 &= \frac{1}{\sqrt{\mathcal{L}}} \sum_{b=1}^{\mathcal{L}} \frac{1}{\sqrt{2}} (\psi_{1,b,\uparrow} - \psi_{1,b,\downarrow}) \\ &= \frac{1}{\sqrt{\mathcal{L}}} \sum_{b=1}^{\mathcal{L}} \frac{1}{\sqrt{2}} (|\uparrow\rangle \otimes c_{b,\downarrow}^\dagger - |\downarrow\rangle \otimes c_{b,\uparrow}^\dagger) \Psi_M^{\mathcal{L}\setminus b}. \end{aligned} \quad (50)$$

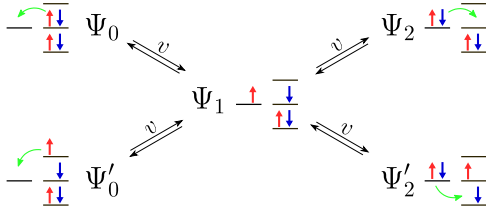


FIG. 7. Schematic representation of the states coupled in the singlet subspace. In the flat-band limit, no other states couple with this subset. The green arrows represent the hopping processes relating states to  $\Psi_1$ .

Making use of Eq. (41) at half-filling ( $M = \mathcal{L}/2$ ), this can also be expressed as

$$\Psi_1 \approx (|\uparrow\rangle \otimes f_{\downarrow}^{\dagger} - |\downarrow\rangle \otimes f_{\uparrow}^{\dagger}) \Psi_M^{\mathcal{L}}. \quad (51)$$

We note that no spin-triplet states are included here.

To find the matrix elements, we make use of the result from Appendix B in the large  $\mathcal{L}$  limit:

$$f_{\uparrow}^{\dagger} f_{\downarrow}^{\dagger} \Psi_M^{\mathcal{L}} \approx \frac{1}{2} \Psi_{M+1}^{\mathcal{L}} + \frac{1}{2} \frac{1}{\mathcal{L}} \sum_{b \neq b'} c_{b\uparrow}^{\dagger} c_{b'\downarrow}^{\dagger} \Psi_M^{\mathcal{L}}. \quad (52)$$

We find, for example,

$$\begin{aligned} \langle \Psi_0 | f_{\uparrow}^{\dagger} d_{\uparrow} | \Psi_1 \rangle &= \langle 0 | (\Psi_{M+1}^{\mathcal{L}})^* (-d_{\uparrow} f_{\uparrow}^{\dagger}) | \uparrow \rangle \otimes f_{\downarrow}^{\dagger} \Psi_M^{\mathcal{L}} \\ &= \langle 0 | d_{\uparrow} | \uparrow \rangle (\Psi_{M+1}^{\mathcal{L}})^* f_{\uparrow}^{\dagger} f_{\downarrow}^{\dagger} \Psi_M^{\mathcal{L}} \\ &\approx 1/2, \end{aligned} \quad (53)$$

and similarly

$$\langle \Psi_0 | f_{\downarrow}^{\dagger} d_{\downarrow} | \Psi_1 \rangle \approx 1/2, \quad (54)$$

giving a total electron hopping matrix element of 1. Other matrix elements can be computed in an analogous way. The effective Hamiltonian in the basis  $\{\Psi_1, \Psi_0, \Psi'_0, \Psi_2, -\Psi'_2\}$  in the large- $\mathcal{L}$  limit is then

$$H_{\text{eff}}^S = \begin{pmatrix} E_1^S & v & v & v & v \\ v & E_0^S & 0 & 0 & 0 \\ v & 0 & E_0^{S'} & 0 & 0 \\ v & 0 & 0 & E_2^S & 0 \\ v & 0 & 0 & 0 & E_2^{S'} \end{pmatrix}. \quad (55)$$

The signs of basis states have been chosen so that the out-of-diagonal matrix elements are all positive (in the sense of having the same sign as  $v$ ). The schematic representation of this Hamiltonian is shown in Fig. 7. If the  $1/\mathcal{L}$  corrections in diagonal elements are neglected (as is valid in the large  $\mathcal{L}$  limit), so that

$$\begin{aligned} E_{02}^S &= -\alpha \frac{\mathcal{L}}{2} + U/2, \\ E_{02}^{S'} &= -\alpha \frac{\mathcal{L}}{2} + 2\alpha + U/2 = E_{02}^S + 2\alpha, \\ E_1^S &= -\alpha \frac{\mathcal{L}}{2} + \alpha, \end{aligned} \quad (56)$$

then the problem simplifies further to a  $3 \times 3$  matrix problem:

$$H_{\text{eff}}^S = \begin{pmatrix} E_1^S & \sqrt{2}v & \sqrt{2}v \\ \sqrt{2}v & E_{02}^S & 0 \\ \sqrt{2}v & 0 & E_{02}^{S'} \end{pmatrix}. \quad (57)$$

The numeric diagonalization of this Hamiltonian produces a result which agrees very well with the DMRG results even for  $\mathcal{L} = 50$ ; see Fig. 6 (bottom panel). Exact matrix elements for any values of  $\mathcal{L}$  and  $M$  are provided in Appendix D.

#### D. Dependence on hybridization strength

We now consider the  $\Gamma$ -dependence of the singlet-doublet excitation energy for different values of  $U$ .

##### 1. Large- $U$ regime

At the particle-hole symmetric point, the lowest eigenvalue of the Hamiltonian  $H_{\text{eff}}^D$  in Eq. (45) is

$$E_D = -\alpha \frac{\mathcal{L} - 1}{2} + \frac{U - \sqrt{16v^2 + (U + 2\alpha)^2}}{4}. \quad (58)$$

The expansion around the  $U \rightarrow \infty$  limit is

$$\begin{aligned} E_D &\approx -\alpha \frac{\mathcal{L}}{2} - 2 \frac{v^2}{U} + \frac{4v^2\alpha}{U^2} + \mathcal{O}(1/U^3) \\ &= -\alpha \frac{\mathcal{L}}{2} - \frac{J}{4} + \frac{J\alpha}{2U} + \mathcal{O}(1/U^3), \end{aligned} \quad (59)$$

where  $J = 8v^2/U$  as defined in Eq. (30). The first term is the energy of the half-filled decoupled bath, Eq. (18). The second term is the trivial linear shift of energies in the Schrieffer-Wolff transformation [75],  $-J/4$ . The third term is the leading order  $J/U$  correction. As expected, it is proportional to  $\alpha$  and  $J$ , and inversely proportional to  $U$  (the energy cost of valence fluctuations), since it is due to the perturbation of the SC state by the hybridization with the impurity.

The lowest eigenvalue of the Hamiltonian  $H_{\text{eff}}^S$  in Eq. (57) in the large- $U$  limit is

$$\begin{aligned} E_S &\approx -\alpha \frac{\mathcal{L} - 2}{2} - \frac{8v^2}{U} + \mathcal{O}(1/U^3) \\ &= -\alpha \frac{\mathcal{L} - 2}{2} - J + \mathcal{O}(1/U^3). \end{aligned} \quad (60)$$

Now we consider the difference, i.e., the Yu-Shiba-Rusinov excitation energy  $E_{\text{YSR}} = E_S - E_D$ . At large  $U$  we then recover the Kondo-limit results from Sec. IV B,

$$E_{\text{YSR}} = \alpha - \frac{3J}{4}, \quad (61)$$

up to  $1/\mathcal{L}$  corrections.

For moderate  $U$  one finds deviations from the simple linear-in- $\Gamma$  behavior, see Fig. 8. The YSR energy at the same  $\Gamma/U$  ratio is found to be *higher*, the lower  $U$  is. The charge fluctuations thus reduce the effects of the exchange coupling (at the same value of  $J$ ). Note that at large  $\Gamma$  the eigenvalue reaches the limiting value of  $E_{\text{edge}} = E^{qp,+} - 2\alpha = (1 + 1/\mathcal{L})\alpha - 2\alpha = -(1 - 1/\mathcal{L})\alpha$  (the ‘‘gap edge’’) with a finite slope, indicating a level crossing. This is the main difference compared with the problem with a finite bandwidth,

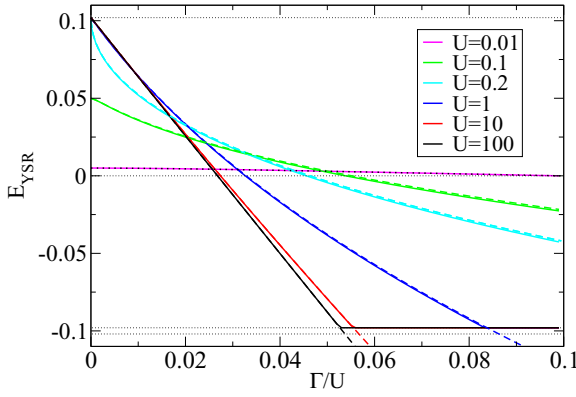


FIG. 8. Excitation energy  $E_{\text{YSR}} = E_S - E_D$  in the flat-band limit for the  $\Delta N = 1$  transitions. Parameters are  $\mathcal{L} = 50$ ,  $\alpha = 0.1$ . Full lines: DMRG results. Dashed lines: analytical calculation. The small deviations are due to the  $1/\mathcal{L}$  correction that for simplicity have not been included here. As discussed in the text, the analytical solution passes the “gap edge” value of  $E_{\text{edge}} = -(1 - 1/\mathcal{L})\alpha$  (lowest dotted black line) with a finite slope. The DMRG solver always converges to the lowest-energy excitation, thus beyond this crossing point the DMRG results remain pinned at  $E_{\text{edge}}$ .

where the subgap state experiences a level repulsion and at large  $\Gamma$  asymptotically approaches the gap edge which is accompanied by a continuous transfer of the spectral weight from the subgap states to the continuum of Bogoliubov excitations [83]. In the flat-band case there is no continuum, only a set of degenerate excitations which do not hybridize with the subgap state, thus the hybridized state can cross this set unperturbed. The nonlinearity in  $\Gamma$  can be obtained by expanding the lowest eigenvalue of  $H_{\text{eff}}^S$  to the next order in  $1/U$ :

$$\begin{aligned} E_S &\approx -\alpha \frac{\mathcal{L} - 2}{2} - \frac{8v^2}{U} + \frac{128v^4 - 32v^2\alpha^2}{U^3} \\ &= -\alpha \frac{\mathcal{L} - 2}{2} - \frac{8\Gamma}{\pi\rho U^2} - \frac{32\frac{\Gamma}{U}[(\pi\rho\alpha)^2 - 4\pi\rho\frac{\Gamma}{U}]}{(\pi\rho U)^3}. \end{aligned} \quad (62)$$

### 2. Small- $U$ limit

We now consider the expansion for small values of  $U$ . For Eq. (58) we find

$$E_D \approx -\alpha \frac{\mathcal{L} - 1}{2} + \frac{U}{4} \left( 1 - \frac{\alpha}{\sqrt{\alpha^2 + 4v^2}} \right) - \frac{\sqrt{\alpha^2 + 4v^2}}{2}. \quad (63)$$

Taking the small- $\Gamma$  limit gives  $E_D \approx -\alpha\mathcal{L}/2$ , thereby fully canceling out the  $U$  dependence.

The lowest eigenvalue of the Hamiltonian  $H_{\text{eff}}^S$  in Eq. (57) in the small- $U$  limit is

$$E_S \approx -\alpha \frac{\mathcal{L} - 2}{2} + \frac{U}{2} \frac{\alpha^2 + 2v^2}{\alpha^2 + 4v^2} - \sqrt{\alpha^2 + 4v^2}. \quad (64)$$

Taking the  $\Gamma \rightarrow 0$  limit, we find  $E_S \approx -\alpha\mathcal{L}/2 + U/2$ . At zero  $\Gamma$ , the excitation energy is

$$\Delta E(\Gamma = 0) = \lim_{\Gamma \rightarrow 0} (E_S - E_D) = U/2, \quad (65)$$

as expected and as seen in Fig. 8. The lowest excitation is not a YSR singlet, but a ABS-like state with a QD in a proximitized state ( $|0\rangle + |2\rangle$  superposition). We note in passing that the order of taking the limits is important; here we took the limit of  $U \rightarrow 0$  followed by  $\Gamma \rightarrow 0$ .

The  $\Gamma$  dependence to lowest order is

$$\Delta E = E_S - E_D \approx \frac{U}{2} - \frac{\Gamma}{\pi\rho\alpha} \left( 1 + \frac{3U}{2\alpha} \right). \quad (66)$$

The energy reduction in the Andreev-bound-state regime is controlled by the  $\Gamma/\alpha$  ratio, a nonzero repulsion  $U$  is merely an order  $U/\alpha$  correction to the prefactor.

### 3. Special case of $U = 2\alpha$

In the limit of  $U = 2\alpha$ , some states in the singlet subspace become degenerate:  $E_{02}^S = E_1^S$ . In this regime, we find the following expansions in the weak hybridization limit:

$$\begin{aligned} E_D &= -\alpha \frac{\mathcal{L}}{2} - \frac{v^2}{2\alpha}, \\ E_S &= -\alpha \frac{\mathcal{L}}{2} - \frac{v^2}{2\alpha} + \alpha - \sqrt{2}v. \end{aligned} \quad (67)$$

This leads to the interesting result that

$$E_S - E_D = \alpha - \sqrt{\frac{2\Gamma}{\pi\rho}}. \quad (68)$$

This square root singularity is indeed observed in the results shown in Fig. 8.

The singular behavior observed at  $U = 2\alpha$  marks the boundary between the regimes of proximitized (Andreev) subgap states for  $U < 2\alpha$  and the Yu-Shiba-Rusinov states for  $U > 2\alpha$ . This is a nontrivial observation because it is generally believed that the cross-over between these two limits is perfectly smooth. In fact, there exists a clear anomaly at  $U = 2\alpha$  in the low- $\Gamma$  limit.

### E. Dependence on gate voltage

The formalism also correctly describes the transitions to different impurity occupancies when  $\epsilon = U/(1/2 - v)$  with  $v \neq 1$ . We find good agreement with the reference DMRG results, see Fig. 9. This is the case even taking the truncated three-dimensional basis from Eq. (45). For  $v$  sufficiently far away from 1, the doublet solution enters the quasicontinuum: the black line in Fig. 9 shoots past the gap edge  $\alpha(1 + 1/\mathcal{L})$ . The true lowest excited state is then a decoupled Bogoliubov quasiparticle sitting at the bottom of the quasicontinuum.

In the large- $U$  limit, the lowest lying eigenstates are

$$\begin{aligned} E_S &\approx -\alpha \frac{\mathcal{L} - 2}{2} + \frac{8v^2}{u(3 + 4v(v - 2))}, \\ E_D &\approx -\alpha \frac{\mathcal{L}}{2} + \frac{2v^2}{u(3 + 4v(v - 2))}, \end{aligned} \quad (69)$$

so that

$$\begin{aligned} \Delta E = E_S - E_D &= \frac{(\mathcal{L} + 1)}{\mathcal{L}}\alpha + \frac{6v^2}{3 + 4v(v - 2)} \\ &\approx \alpha - \frac{3J}{4}, \end{aligned} \quad (70)$$

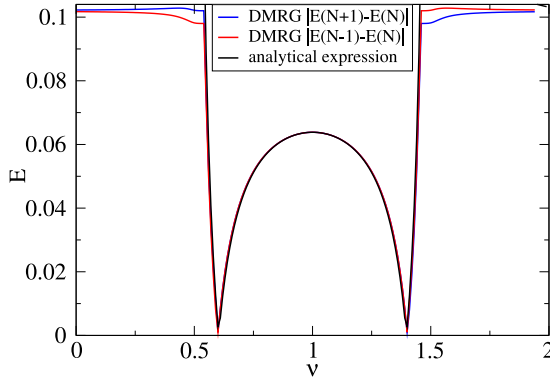


FIG. 9. YSR subgap state dispersion (positive frequency branch) in the flat-band limit. The lineshape corresponds to the conventional YSR loops. Parameters are  $U = 100$ ,  $\mathcal{L} = 50$ ,  $\Gamma/U = 0.01$ ,  $\epsilon = U(1/2 - v)$ , where  $v$  controls the impurity filling.

where we noted that away from half filling, the Kondo exchange coupling is

$$J = \frac{2v^2}{-\epsilon} + \frac{2v^2}{U + \epsilon} = \frac{1}{4v(2-v) - 3} \frac{8v^2}{U}. \quad (71)$$

As expected, to first order in  $1/U$ , the only effect of departure from the particle-hole asymmetry is the modified value of the Kondo exchange. The leading correction is of order  $\alpha J/U$ , as found in the previous section.

## V. COMPARISON TO THE BCS ZERO-BANDWIDTH APPROXIMATION

A commonly used approximation in QD-SC models is the ZBW limit of BCS, where the SC is modeled by a single level with mean-field pairing interaction [84–87]. Here we show that this description is equivalent to the RM in the  $\gamma \rightarrow 0$  limit. Consider the ZBW Hamiltonian

$$H = \epsilon(\hat{n} - 1) + U\hat{n}_\uparrow\hat{n}_\downarrow + v \sum_{i,\sigma} (f_\sigma^\dagger d_\sigma + d_\sigma^\dagger f_\sigma) - \Delta(f_\uparrow^\dagger f_\downarrow^\dagger + \text{H.c.}). \quad (72)$$

In the doublet subspace with the basis states  $\{d_\uparrow^\dagger, d_\uparrow^\dagger f_\uparrow^\dagger f_\downarrow^\dagger, f_\uparrow^\dagger, d_\downarrow^\dagger d_\uparrow^\dagger f_\uparrow^\dagger\}$  (applied to the zero occupancy vacuum state) one finds the following matrix representation:

$$H_{\text{ZBW}}^D = \begin{pmatrix} 0 & -\Delta & v & 0 \\ -\Delta & 0 & 0 & -v \\ v & 0 & -\epsilon & 0 \\ 0 & -v & 0 & U + \epsilon \end{pmatrix}. \quad (73)$$

Alternatively, one may work in the basis

$$\begin{aligned} (d_\uparrow^\dagger + d_\uparrow^\dagger f_\uparrow^\dagger f_\downarrow^\dagger)/\sqrt{2} &= d_\uparrow^\dagger(1 + f_\uparrow^\dagger f_\downarrow^\dagger)/\sqrt{2}, \\ (d_\uparrow^\dagger - d_\uparrow^\dagger f_\uparrow^\dagger f_\downarrow^\dagger)/\sqrt{2} &= d_\uparrow^\dagger(1 - f_\uparrow^\dagger f_\downarrow^\dagger)/\sqrt{2}, \\ f_\uparrow^\dagger, & \quad d_\uparrow^\dagger d_\downarrow^\dagger f_\uparrow^\dagger, \end{aligned}$$

where the matrix representation is

$$H_{\text{ZBW}}^D = \begin{pmatrix} -\Delta & 0 & v/\sqrt{2} & -v/\sqrt{2} \\ 0 & +\Delta & v/\sqrt{2} & v/\sqrt{2} \\ v/\sqrt{2} & v/\sqrt{2} & -\epsilon & 0 \\ -v/\sqrt{2} & v/\sqrt{2} & 0 & U + \epsilon \end{pmatrix}, \quad (74)$$

which is equivalent to  $H_{\text{eff}}^D$  in Eq. (42) up to a trivial shift of all diagonal elements. The combination  $(1 + f_\uparrow^\dagger f_\downarrow^\dagger)/\sqrt{2}$  represents a Cooper-pair state, while the combination  $(1 - f_\uparrow^\dagger f_\downarrow^\dagger)/\sqrt{2}$  represents a two-quasiparticles state with the energy cost of  $2\Delta$ .

In the singlet subspace, we work in the basis (the signs are chosen to produce positive signs for the out-of-diagonal matrix elements)

$$\begin{aligned} (d_\uparrow^\dagger f_\downarrow^\dagger - d_\downarrow^\dagger f_\uparrow^\dagger)/\sqrt{2}, & \quad (1 + f_\uparrow^\dagger f_\downarrow^\dagger)/\sqrt{2}, \\ -(1 - f_\uparrow^\dagger f_\downarrow^\dagger)/\sqrt{2}, & \quad d_\uparrow^\dagger d_\downarrow^\dagger(1 + f_\uparrow^\dagger f_\downarrow^\dagger)/\sqrt{2}, \\ d_\uparrow^\dagger d_\downarrow^\dagger(1 - f_\uparrow^\dagger f_\downarrow^\dagger)/\sqrt{2}, & \end{aligned}$$

where the matrix takes the following form:

$$H_{\text{ZBW}}^S = \begin{pmatrix} 0 & v & v & v & v \\ v & -\Delta - \epsilon & 0 & 0 & 0 \\ v & 0 & \Delta - \epsilon & 0 & 0 \\ v & 0 & 0 & -\Delta + U + \epsilon & 0 \\ v & 0 & 0 & 0 & \Delta + U + \epsilon \end{pmatrix}. \quad (75)$$

Up to a trivial energy shift, this is exactly the same as  $H_{\text{eff}}^S$  from Eq. (55).

The equivalence between the models is exact in the ZBW limit  $\gamma \rightarrow 0$ , when  $\alpha$  plays the role of excitation energy gap, akin to  $\Delta$  in BCS. The demonstration of this equivalence is one of the key results of this work.

## VI. CONCLUSION

Even though superconductivity and Bose-Einstein condensation are apparently quite different states of matter, they emerge as a result of the same attractive pairing interaction in the opposite limits of pairing strength. When a system with pairing interaction is coupled to a magnetic impurity, it induces discrete singlet states inside the SC gap. We find that the subgap states persist throughout the weak to strong pairing crossover, and we furthermore show that their nature remains qualitatively the same. The differences are limited to the scaling of hybridization strength and excitation gap, both due to the decreasing importance of bath kinetic energy with increased pairing.

In the limit of strong pairing interaction the kinetic energy term can be omitted. The single-particle levels in the bath are then degenerate, which lets us obtain a flat-band Hamiltonian in the reduced Hilbert space spanned by just a few many-particle states connected by the Hamiltonian. The BEC limit of the problem is in this sense analytically solvable, and we show that the results agree very well with exact calculations. We also show that the flat-band Hamiltonian in the limit of

large system is formally exactly equivalent to the BCS zero bandwidth approximation.

ZBW approximations and similar toy models are very commonly applied when modeling QDs coupled to SCs [87–91]. Our result explains their surprisingly strong predictive power and thus provides a solid foundation for their application in this context. Typically the argument for using the ZBW approximation is that a single level at the gap edge is sufficient to encompass the important phenomena, because the SC has a diverging density of states at the gap edge and because these near-edge are the most important for the subgap state formation: in fact, the subgap state weight originates precisely from the depletion of the spectral weight from the superconducting coherence peaks. The higher excited states largely remain unperturbed by the impurity, and their small contributions can be discarded. We find that this is a very reasonable approximation in a variety of situations.

Due to its simplicity, the flat-band model can be straightforwardly extended in various ways. To accurately describe mesoscopic SC islands, it is important to take into account the Coulomb repulsion between the island electrons [52]. This can be done by augmenting the model with a charging energy term  $E_C \hat{n}_{SC}^2$ . Because the RM conserves particle number we are operating in the canonical ensemble, thus implementing such operator is very simple and it is straightforward to extend the effective flat-band model by adding  $E_C$  to appropriate diagonal matrix elements. For a problem with a single SC bath, this merely reduces the energy scale for charge fluctuations from  $U/2$  to  $U/2 + E_C$  [50–52]. The Zeeman splitting can also be trivially included in the flat-band model. Additional triplet (and quadruplet) states that become relevant at large magnetic fields can also be included in consideration.

The analytical approach can also be extended to multi-channel impurity problems. These have additional degrees of freedom, namely the occupation number differences between channels (i.e., the distribution of Cooper pairs between the two superconductors). An appropriate linear combination of such states corresponds to well defined phase differences which would appear in the equivalent BCS formalism, while a charging term would induce phase fluctuations. We will pursue this direction in our future work.

## ACKNOWLEDGMENTS

We acknowledge discussions with Gorm Steffensson, Jens Paaske, Virgil V. Baran, and Martin Žonda. We acknowledge the support of the Slovenian Research Agency (ARRS) under Grants No. P1-0044, No. P1-0416, and No. J1-3008.

## APPENDIX A: EIGENENERGY CALCULATION

Summing Eq. (6) over  $i, j$  in the set  $\mathcal{U}$  we obtain

$$[B, B^\dagger] = 1 - \frac{1}{\mathcal{U}} \hat{N}, \quad (\text{A1})$$

where  $\hat{N} = \sum_i^{\mathcal{U}} \hat{n}_i$  is the total number of electrons in the unblocked levels.

In this Appendix we evaluate  $B^\dagger B$  on state  $|M\rangle = (B^\dagger)^M |0\rangle$ . By repeatedly commuting  $B^\dagger$  and  $B$  we find

$$\begin{aligned} B^\dagger B |M\rangle &= (B^\dagger B) (B^\dagger)^M |0\rangle \\ &= \left[ B^\dagger \left( B^\dagger B + 1 - \frac{1}{\mathcal{U}} \hat{N} \right) (B^\dagger)^{M-1} \right] |0\rangle \\ &= \left[ (B^\dagger)^2 B (B^\dagger)^{M-1} + \left( 1 - \frac{2(M-1)}{\mathcal{U}} \right) (B^\dagger)^M \right] |0\rangle \\ &= \left[ (B^\dagger)^3 B (B^\dagger)^{M-2} + \left( 1 - \frac{2(M-2)}{\mathcal{U}} \right) (B^\dagger)^M \right. \\ &\quad \left. + \left( 1 - \frac{2(M-1)}{\mathcal{U}} \right) (B^\dagger)^M \right] |0\rangle \\ &= \left[ \sum_{m=1}^M \left( 1 - \frac{2(m-1)}{\mathcal{U}} \right) \right] |M\rangle = c_M |M\rangle, \quad (\text{A2}) \end{aligned}$$

with

$$c_M = \frac{(1 + \mathcal{U} - M)M}{\mathcal{U}}. \quad (\text{A3})$$

## APPENDIX B: ACTION OF CREATION OPERATORS ON $\Psi_M^{\mathcal{L}}$

In this Appendix we discuss the action of fermionic operators on the eigenstates  $\Psi_M^{\mathcal{L}, \mathcal{U}}$  of the Richardson's model. This defines the relations between the states from subspaces distinguished by the different number  $M$  of Cooper pairs. The subsectors differing by  $\Delta M = \pm 1$  are coupled due to the Cooper-pair-breaking property of the exchange interaction induced by the presence of the magnetic impurity. The relations derived in the following provide the full set of algebraic relations required to determine the coupling between the accessible states and all matrix elements in the flat-band limit.

### 1. Single-quasiparticle state

In this section the number of levels is fixed to  $\mathcal{L}$ . When a single superscript is indicated for brevity, the number indicates the number of unblocked levels, i.e.,  $\Psi_M^{\mathcal{L}} \equiv \Psi_M^{\mathcal{L}, \mathcal{U}}$ . When no superscript is indicated, all levels are unblocked, i.e.,  $\Psi_M \equiv \Psi_M^{\mathcal{L}, \mathcal{L}}$ .

Let us consider the spin-doublet state

$$\psi_\sigma = f_\sigma^\dagger \Psi_M^{\mathcal{L}, \mathcal{L}} = \frac{1}{\sqrt{\mathcal{L}}} \sum_{b=1}^{\mathcal{L}} c_{b, \sigma}^\dagger \Psi_M^{\mathcal{L}, \mathcal{L}}, \quad (\text{B1})$$

with  $\Psi_M^{\mathcal{L}, \mathcal{L}}$  being the normalized eigenstate for  $M$  Cooper pairs in a system with  $\mathcal{L}$  levels, all of them unblocked. The application of the creation operator creates a superposition of states with one blocked level indexed by  $b$ . This state is thus spanned by the following *orthonormal* set of  $\mathcal{L}$  eigenstates of the SC bath:

$$\phi_{b\sigma} = c_{b, \sigma}^\dagger \Psi_M^{\mathcal{L}, \mathcal{L} \setminus b}, \quad (\text{B2})$$

where  $\mathcal{L} \setminus b$  in the superscript of  $\Psi$  indicates that the level  $b$  is blocked. If all levels are equal, then so are the coefficients, thus

$$\psi_\sigma = C \frac{1}{\sqrt{\mathcal{L}}} \sum_{b=1}^{\mathcal{L}} \phi_{b\sigma}. \quad (\text{B3})$$



Let us now fix the proportionality constant  $C$ :

$$\langle \psi_\sigma | \psi_\sigma \rangle = \langle \Psi_M^\mathcal{L} | f_\sigma^\dagger f_\sigma^\dagger | \Psi_M^\mathcal{L} \rangle = 1 - \langle \Psi_M^\mathcal{L} | f_\sigma^\dagger f_\sigma | \Psi_M^\mathcal{L} \rangle = C^2. \quad (\text{B4})$$

We expand in the site basis:

$$\begin{aligned} f_\sigma^\dagger f_\sigma &= \frac{1}{\mathcal{L}} \sum_{i,j} c_{i,\sigma}^\dagger c_{j,\sigma} = \frac{1}{\mathcal{L}} \sum_i \hat{n}_{i,\sigma} + \frac{1}{\mathcal{L}} \sum_{i \neq j} c_{i,\sigma}^\dagger c_{j,\sigma} \\ &= \frac{\hat{N}_\sigma}{\mathcal{L}} + \frac{1}{\mathcal{L}} \sum_{i \neq j} c_{i,\sigma}^\dagger c_{j,\sigma}. \end{aligned} \quad (\text{B5})$$

The first term gives  $M/\mathcal{L}$ . The second gives zero, because when applied to the ket it produces a linear combination of terms which all contain singly occupied levels, and such a state is orthogonal to  $\Psi_M^\mathcal{L}$  in the bra. Finally,

$$C^2 = 1 - \frac{M}{\mathcal{L}} = \frac{\mathcal{L} - M}{\mathcal{L}}. \quad (\text{B6})$$

We conclude that

$$\psi_\sigma = f_\sigma^\dagger \Psi_M^{\mathcal{L},\mathcal{L}} = \sqrt{\frac{\mathcal{L} - M}{\mathcal{L}}} \frac{1}{\sqrt{\mathcal{L}}} \sum_b c_{b,\sigma}^\dagger \Psi_M^{\mathcal{L},\mathcal{L} \setminus b}. \quad (\text{B7})$$

This expression is exact. For  $M \rightarrow 0$ , in the absence of any Cooper pairs, the prefactor becomes equal to 1, since the electron can be added to any level. For  $M \rightarrow \mathcal{L}$ , the prefactor tends to 0, since there are only a few levels available to accommodate the additional electron. Finally, for half filling the prefactor becomes  $1/\sqrt{2}$ , thus

$$\psi_\sigma = f_\sigma^\dagger \Psi_{\mathcal{L}/2}^{\mathcal{L},\mathcal{L}} = \frac{1}{\sqrt{2}} \frac{1}{\sqrt{\mathcal{L}}} \sum_b c_{b,\sigma}^\dagger \Psi_{\mathcal{L}/2}^{\mathcal{L} \setminus b}. \quad (\text{B8})$$

Note that this state  $\psi_\sigma$  is *not* normalized to 1.

In the same way one derives

$$\psi'_\sigma = f_\sigma \Psi_M^{\mathcal{L},\mathcal{L}} = (-1)^\sigma \sqrt{\frac{M}{\mathcal{L}}} \frac{1}{\sqrt{\mathcal{L}}} \sum_b c_{b,\sigma}^\dagger \Psi_{M-1}^{\mathcal{L},\mathcal{L} \setminus b}, \quad (\text{B9})$$

where  $(-1)^\uparrow = -1$  and  $(-1)^\downarrow = 1$ . This expression is exact. It simplifies at half filling to

$$\psi'_\sigma = (-1)^\sigma f_\sigma \Psi_{\mathcal{L}/2}^{\mathcal{L},\mathcal{L}} = \frac{1}{\sqrt{2}} \frac{1}{\sqrt{\mathcal{L}}} \sum_b c_{b,\sigma}^\dagger \Psi_{\mathcal{L}/2-1}^{\mathcal{L} \setminus b}, \quad (\text{B10})$$

The sign factor is due to the order convention of spin-up and spin-down operators in the hard-core boson operators  $A_i$ .

## 2. Two-quasiparticle state

The other state of interest is the spin-singlet state

$$\begin{aligned} \psi_2 &= f_\uparrow^\dagger f_\downarrow^\dagger \Psi_M^\mathcal{L} \\ &= \frac{1}{\mathcal{L}} \sum_{i,j} c_{i\uparrow}^\dagger c_{j\downarrow}^\dagger \Psi_M^\mathcal{L} \\ &= \frac{1}{\mathcal{L}} \sum_i A_i^\dagger \Psi_M^\mathcal{L} + \frac{1}{\mathcal{L}} \sum_{b \neq b'} c_{b\uparrow}^\dagger c_{b'\downarrow}^\dagger \Psi_M^\mathcal{L} \\ &= \frac{1}{\sqrt{\mathcal{L}}} B^\dagger \Psi_M^\mathcal{L} + \frac{1}{\mathcal{L}} \sum_{b \neq b'} c_{b\uparrow}^\dagger c_{b'\downarrow}^\dagger \Psi_M^\mathcal{L}. \end{aligned} \quad (\text{B11})$$

We have

$$B^\dagger \Psi_M^\mathcal{L} = B^\dagger \mathcal{N}_M |M\rangle = \mathcal{N}_M |M+1\rangle = \frac{\mathcal{N}_M}{\mathcal{N}_{M+1}} \Psi_{M+1}^\mathcal{L}. \quad (\text{B12})$$

The normalization factors  $\mathcal{N}_M$  are evaluated in Appendix C. The states with two blocked levels are spanned by the *orthonormal* set of  $\mathcal{L}^2 - \mathcal{L} = \mathcal{L}(\mathcal{L} - 1)$  states (for  $b \neq b'$ ),

$$\phi_{bb'} = c_{b,\uparrow}^\dagger c_{b',\downarrow}^\dagger \Psi_M^{\mathcal{L},\mathcal{L} \setminus b,b'}. \quad (\text{B13})$$

We thus have

$$\frac{1}{\mathcal{L}} \sum_{b \neq b'} c_{b\uparrow}^\dagger c_{b'\downarrow}^\dagger \Psi_M^\mathcal{L} = C \frac{1}{\sqrt{\mathcal{L}(\mathcal{L} - 1)}} \sum_{b \neq b'} \phi_{bb'}, \quad (\text{B14})$$

with a proportionality constant  $C$  that needs to be determined. For that purpose, we compute the norm:

$$C^2 = \frac{1}{\mathcal{L}^2} \sum_{b \neq b', c \neq c'} \langle \Psi_M^\mathcal{L} | c_{c'\downarrow} c_{c\uparrow} c_{b\uparrow}^\dagger c_{b'\downarrow}^\dagger | \Psi_M^\mathcal{L} \rangle. \quad (\text{B15})$$

Only the terms with  $c = b$  and  $c' = b'$  contribute, otherwise the states are orthogonal. Now

$$c_{b'\downarrow} c_{b\uparrow} c_{b\uparrow}^\dagger c_{b'\downarrow}^\dagger = 1 - \hat{n}_{b\uparrow} - \hat{n}_{b'\downarrow} + \hat{n}_{b\uparrow} \hat{n}_{b'\downarrow}. \quad (\text{B16})$$

We need to handle the restriction to  $b \neq b'$  carefully, noting that  $\sum_{b \neq b'} 1 = \mathcal{L}(\mathcal{L} - 1)$ ,  $\sum_{b \neq b'} \hat{n}_{b\sigma} = N_\sigma(\mathcal{L} - 1)$ , and

$$\sum_{b \neq b'} \hat{n}_{b\uparrow} \hat{n}_{b'\downarrow} = \sum_{b,b'} \hat{n}_{b\uparrow} \hat{n}_{b'\downarrow} - \sum_b \hat{n}_{b\uparrow} \hat{n}_{b\downarrow} = \hat{N}_\uparrow \hat{N}_\downarrow - \sum_b \hat{P}_{2,b}. \quad (\text{B17})$$

The operator  $\hat{P}_2 = \sum_b \hat{P}_{2,b}$  counts the number of pairs in the system, therefore  $\langle \Psi_M | \hat{P}_2 | \Psi_M \rangle = M$ . Collecting all terms we then find

$$\begin{aligned} C^2 &= \frac{1}{\mathcal{L}^2} \langle \Psi_M^\mathcal{L} | [\mathcal{L}(\mathcal{L} - 1) - (\mathcal{L} - 1)\hat{N}_\uparrow \\ &\quad - (\mathcal{L} - 1)\hat{N}_\downarrow + \hat{N}_\uparrow \hat{N}_\downarrow - \hat{P}_2] | \Psi_M^\mathcal{L} \rangle \\ &= \frac{(\mathcal{L} - M)(\mathcal{L} - M - 1)}{\mathcal{L}^2}. \end{aligned} \quad (\text{B18})$$

For  $M = 0$ , the factor  $C^2 = 1 - \frac{1}{\mathcal{L}}$ , which goes to 1 in the large- $\mathcal{L}$  limit. In the opposite limit of  $M = \mathcal{L}$ , it is zero. Finally, for half filling, it tends to  $C^2 = 1/2$  in the large- $\mathcal{L}$  limit.

We write  $\psi_2$  in the form

$$\begin{aligned} \psi_2 &= f_\uparrow^\dagger f_\downarrow^\dagger \Psi_M^\mathcal{L} = \frac{\sqrt{(1+M)(\mathcal{L}-M)}}{\mathcal{L}} \Psi_{M+1}^\mathcal{L} \\ &\quad + \frac{\sqrt{(\mathcal{L}-M)(\mathcal{L}-M-1)}}{\mathcal{L}} \frac{1}{\sqrt{\mathcal{L}(\mathcal{L}-1)}} \sum_{b \neq b'} \phi_{bb'}. \end{aligned} \quad (\text{B19})$$

This expression is exact. There is an overall  $\sqrt{\mathcal{L}-M}$  factor. The relative importance of the first and the second term scale as  $\sqrt{M}$  and  $\sqrt{\mathcal{L}-M}$ , respectively, up to  $1/\mathcal{L}$  corrections.

For  $M = \mathcal{L}/2$ , we finally find

$$\begin{aligned} \psi_2 &= f_\uparrow^\dagger f_\downarrow^\dagger \Psi_M^\mathcal{L} = \frac{1}{2} \sqrt{\frac{2+\mathcal{L}}{\mathcal{L}}} \Psi_{M+1}^\mathcal{L} \\ &\quad + \frac{1}{2} \sqrt{\frac{\mathcal{L}-2}{\mathcal{L}-1}} \frac{1}{\mathcal{L}} \sum_{b \neq b'} c_{b\uparrow}^\dagger c_{b'\downarrow}^\dagger \Psi_M^{\mathcal{L} \setminus b,b'}. \end{aligned} \quad (\text{B20})$$

Note that for large  $\mathcal{L}$  both square roots tend toward 1. The states with two blocked levels are orthogonal to  $\Psi_{M+1}^{\mathcal{L}}$  states. Hence,

$$\langle \psi_2 | \psi_2 \rangle = \frac{(1+M)(\mathcal{L}-M)}{\mathcal{L}^2} + \frac{(\mathcal{L}-M)(\mathcal{L}-M-1)}{\mathcal{L}^2} = \frac{\mathcal{L}-M}{\mathcal{L}}. \quad (\text{B21})$$

For  $M = \mathcal{L}/2$ , this gives

$$\langle \psi_2 | \psi_2 \rangle = \frac{1}{2}. \quad (\text{B22})$$

The state  $\psi_2 = f_{\uparrow}^{\dagger} f_{\downarrow}^{\dagger} \Psi_M^{\mathcal{L}}$  is thus not normalized to 1.

In an analogous way one calculates

$$\psi_2' = f_{\downarrow} f_{\uparrow} \Psi_M^{\mathcal{L}} = \frac{\sqrt{M(1+\mathcal{L}-M)}}{\mathcal{L}} \Psi_{M-1}^{\mathcal{L}} - \frac{\sqrt{M(M-1)}}{\mathcal{L}} \frac{1}{\sqrt{\mathcal{L}(\mathcal{L}-1)}} \sum_{b \neq b'} \phi_{bb'}, \quad (\text{B23})$$

with  $\phi_{bb'} = c_{b,\uparrow}^{\dagger} c_{b',\downarrow}^{\dagger} \Psi_{M-2}^{\mathcal{L} \setminus b, b'}$ . This expression is exact. At half filling, it simplifies to

$$\psi_2' = f_{\downarrow} f_{\uparrow} \Psi_{\mathcal{L}/2}^{\mathcal{L}} = \frac{1}{2} \sqrt{\frac{2+\mathcal{L}}{\mathcal{L}}} \Psi_{\mathcal{L}/2-1}^{\mathcal{L}} - \frac{1}{2} \sqrt{\frac{\mathcal{L}-2}{\mathcal{L}-1}} \frac{1}{\mathcal{L}} \sum_{b \neq b'} \phi_{bb'}, \quad (\text{B24})$$

with the same prefactors as for  $\psi_2$ .

### APPENDIX C: EVALUATION OF NORMALIZATION $\mathcal{N}_M$

We fix  $\mathcal{N}_M$  from the condition

$$\langle \Psi_M | \Psi_M \rangle = \mathcal{N}_M^2 \langle M | M \rangle = 1. \quad (\text{C1})$$

We write

$$d_M = \langle M | M \rangle = \langle 0 | B^M (B^{\dagger})^M | 0 \rangle, \quad (\text{C2})$$

so that  $\mathcal{N}_M = (d_M)^{-1/2}$ . Clearly  $d_1 = 1$  and  $\mathcal{N}_1 = 1$ .

Recall Eq. (A2),  $B^{\dagger} B | M \rangle = c_M | M \rangle$ . This can also be expressed as  $B | M \rangle = c_M | M-1 \rangle$ . Thus, we find

$$\begin{aligned} d_M &= \langle M | M \rangle = \langle M-1 | B | M \rangle \\ &= c_M \langle M-1 | M-1 \rangle = c_M d_{M-1}. \end{aligned} \quad (\text{C3})$$

The solution of this recursion equation is

$$d_M = (-U)^{-M} (1)_M (-U)_M, \quad (\text{C4})$$

where  $(a)_n = \Gamma(a+n)/\Gamma(a)$  is the Pochhammer symbol. At half filling  $U = \mathcal{L}$  and  $M = \mathcal{L}/2$ , we find

$$d_{\mathcal{L}/2} = \frac{\mathcal{L}!}{\sqrt{\mathcal{L}^{\mathcal{L}}}}. \quad (\text{C5})$$

Furthermore, for  $U = \mathcal{L}$  one has

$$\frac{\mathcal{N}_M^2}{\mathcal{N}_{M+1}^2} = \frac{d_{M+1}}{d_M} = \frac{(1+M)(\mathcal{L}-M)}{\mathcal{L}}. \quad (\text{C6})$$

### APPENDIX D: REFERENCE CALCULATION

The method presented in Sec. IV is exact, but for clarity we have presented in that section only simplified results obtained in the  $\mathcal{L} \rightarrow \infty$  limit at half-filling. Below are the exact expressions for  $H_{\text{eff}}^D$  and  $H_{\text{eff}}^S$ :

$$H_{\text{eff}}^D = \begin{pmatrix} E_1^D & 0 & v\sqrt{\frac{\mathcal{L}-M}{\mathcal{L}}} & -v\sqrt{\frac{M}{\mathcal{L}}} \\ 0 & E_1^{D'} & v\sqrt{\frac{M}{\mathcal{L}}} & v\sqrt{\frac{\mathcal{L}-M}{\mathcal{L}}} \\ v\sqrt{\frac{\mathcal{L}-M}{\mathcal{L}}} & v\sqrt{\frac{M}{\mathcal{L}}} & E_0^D & 0 \\ -v\sqrt{\frac{M}{\mathcal{L}}} & v\sqrt{\frac{\mathcal{L}-M}{\mathcal{L}}} & 0 & E_2^D \end{pmatrix}, \quad (\text{D1})$$

$$H_{\text{eff}}^S = \begin{pmatrix} E_1^S & v\sqrt{\frac{2(M+1)}{\mathcal{L}}} & v\sqrt{\frac{2(\mathcal{L}-M-1)}{\mathcal{L}}} & v\sqrt{\frac{2(\mathcal{L}-M)}{\mathcal{L}}} & v\sqrt{\frac{2M}{\mathcal{L}}} \\ v\sqrt{\frac{2(M+1)}{\mathcal{L}}} & E_0^S & 0 & 0 & 0 \\ v\sqrt{\frac{2(\mathcal{L}-M-1)}{\mathcal{L}}} & 0 & E_0^{S'} & 0 & 0 \\ v\sqrt{\frac{2(\mathcal{L}-M)}{\mathcal{L}}} & 0 & 0 & E_2^S & 0 \\ v\sqrt{\frac{2M}{\mathcal{L}}} & 0 & 0 & 0 & E_2^{S'} \end{pmatrix}. \quad (\text{D2})$$

We provide a Mathematica notebook with these definitions, as well as a corresponding input file for the DMRG solver, as Supplemental Material [53].

- [1] J. Bardeen, L. N. Cooper, and J. R. Schrieffer, Microscopic theory of superconductivity, *Phys. Rev.* **106**, 162 (1957).  
 [2] R. Micnas, J. Ranninger, and S. Robaszkiewicz, Superconductivity in narrow-band systems with local nonretarded interactions, *Rev. Mod. Phys.* **62**, 113 (1990).

- [3] M. Tinkham, *Introduction to Superconductivity*, 2nd ed. (Dover Publications, Mineola, NY, 2004).  
 [4] R. Meservey, P. M. Tedorow, and P. Fulde, Magnetic Field Splitting of the Quasiparticle States in Superconducting Aluminum Films, *Phys. Rev. Lett.* **25**, 1270 (1970).

- [5] Y. Cao, V. Fatemi, S. Fang, K. Watanabe, T. T. Chi, E. Kaxiras, and P. Jarillo-Herrero, Unconventional superconductivity in magic-angle graphene superlattices, *Nature (London)* **556**, 43 (2018).
- [6] J. M. Park, Y. Cao, K. Watanabe, T. Taniguchi, and P. Jarillo-Herrero, Tunable strongly coupled superconductivity in magic-angle twisted trilayer graphene, *Nature (London)* **590**, 249 (2021).
- [7] Y. Nakagawa, Y. Kasahara, T. Nomoto, R. Arita, T. Nojima, and Y. Iwasa, Gate-controlled BCS-BEC crossover in a two-dimensional superconductor, *Science* **372**, 190 (2021).
- [8] A. Bohr, B. R. Mottelson, and D. Pines, Possible analogy between the excitation spectra of nuclei and those of the superconducting metallic state, *Phys. Rev.* **110**, 936 (1958).
- [9] A. Migdal, Superfluidity and the moments of inertia of nuclei, *Nucl. Phys.* **13**, 655 (1959).
- [10] S. T. Belyaev, On the nature of the first excited states of even-even spherical nuclei, *JETP Letters* **12**, 968 (1961).
- [11] R. W. Richardson and N. Sherman, Exact eigenstates of the pairing-force Hamiltonian, *Nucl. Phys.* **52**, 221 (1964).
- [12] V. Zelevinsky and A. Volya, Nuclear pairing: New perspectives, *Phys. At. Nucl.* **66**, 1781 (2003).
- [13] D. J. Dean and M. Hjorth-Jensen, Pairing in nuclear systems: From neutron stars to finite nuclei, *Rev. Mod. Phys.* **75**, 607 (2003).
- [14] P. Nozières and S. Schmitt-Rink, Bose condensation in an attractive fermion gas: From weak to strong coupling superconductivity, *J. Low Temp. Phys.* **59**, 195 (1985).
- [15] S. Jochim, M. Bartenstein, A. Altmeyer, G. Hendl, S. Riedl, C. Chin, J. H. Denschlag, and R. Grimm, Bose-Einstein condensation of molecules, *Science* **302**, 2101 (2003).
- [16] M. Greiner, C. A. Regal, and D. S. Jin, Emergence of a molecular Bose-Einstein condensate from a fermi gas, *Nature (London)* **426**, 537 (2003).
- [17] M. W. Zwierlein, C. A. Stan, C. H. Schunck, S. M. F. Raupach, S. Gupta, Z. Hadzibabic, and W. Ketterle, Observation of Bose-Einstein Condensation of Molecules, *Phys. Rev. Lett.* **91**, 250401 (2003).
- [18] M. Bartenstein, A. Altmeyer, S. Riedl, S. Jochim, C. Chin, J. H. Denschlag, and R. Grimm, Collective Excitations of a Degenerate Gas at the BEC-BCS Crossover, *Phys. Rev. Lett.* **92**, 203201 (2004).
- [19] W. Ketterle and M. W. Zwierlein, Making, probing and understanding ultracold fermi gases, in *Ultracold Fermi Gases, Proceedings of the International School of Physics “Enrico Fermi,” Course CLXIV, Varenna, 20–30 June 2006*, edited by M. Inguscio, W. Ketterle, and C. Salomon (IOS Press, Amsterdam, 2008).
- [20] D. V. Averin and Y. V. Nazarov, Single-Electron Charging of a Superconducting Island, *Phys. Rev. Lett.* **69**, 1993 (1992).
- [21] M. T. Tuominen, J. M. Hergenrother, T. S. Tighe, and M. Tinkham, Experimental Evidence for Parity-Based  $2e$  Periodicity in a Superconducting Single-Electron Tunneling Transistor, *Phys. Rev. Lett.* **69**, 1997 (1992).
- [22] T. M. Eiles, J. M. Martinis, and M. H. Devoret, Even-Odd Asymmetry of a Superconductor Revealed by the Coulomb Blockade of Andreev Reflection, *Phys. Rev. Lett.* **70**, 1862 (1993).
- [23] J. von Delft, A. D. Zaikin, D. S. Golubev, and W. Tichy, Parity-Affected Superconductivity in Ultrasmall Metallic Grains, *Phys. Rev. Lett.* **77**, 3189 (1996).
- [24] J. von Delft and D. Ralph, Spectroscopy of discrete energy levels in ultrasmall metallic grains, *Phys. Rep.* **345**, 61 (2001).
- [25] S. D. Franceschi, L. Kouwenhoven, C. Schönenberger, and W. Wernsdorfer, Hybrid superconductor-quantum dot devices, *Nat. Nanotechnol.* **5**, 703 (2010).
- [26] P. Krogstrup, N. L. B. Ziino, W. Chang, S. M. Albrecht, M. H. Madsen, E. Johnson, J. Nygård, C. M. Marcus, and T. S. Jespersen, Epitaxy of semiconductor-superconductor nanowires, *Nat. Mater.* **14**, 400 (2015).
- [27] M. Randeria and E. Taylor, Crossover from Bardeen-Cooper-Schrieffer to Bose-Einstein condensation and the unitary Fermi gas, *Annu. Rev. Condens. Matter Phys.* **5**, 209 (2014).
- [28] L. Yu, Bound state in superconductors with paramagnetic impurities, *Acta Phys. Sin.* **21**, 75 (1965).
- [29] H. Shiba, Classical spins in superconductors, *Prog. Theor. Phys.* **40**, 435 (1968).
- [30] A. I. Rusinov, Superconductivity near a paramagnetic impurity, *Zh. Eksp. Teor. Fiz. Pisma Red.* **9**, 146 (1968) [*JETP Lett.* **9**, 85 (1969)].
- [31] H. Shiba, A Hartree-Fock theory of transition-metal impurities in a superconductor, *Prog. Theor. Phys.* **50**, 50 (1973).
- [32] A. Sakurai, Comments on superconductors with magnetic impurities, *Prog. Theor. Phys.* **44**, 1472 (1970).
- [33] T. Matsura, The effects of impurities on superconductors with Kondo effect, *Prog. Theor. Phys.* **57**, 1823 (1977).
- [34] A. Yazdani, B. A. Jones, C. P. Lutz, M. F. Crommie, and D. M. Eigler, Probing the local effects of magnetic impurities on superconductivity, *Science* **275**, 1767 (1997).
- [35] A. V. Balatsky, I. Vekhter, and J.-X. Zhu, Impurity-induced states in conventional and unconventional superconductors, *Rev. Mod. Phys.* **78**, 373 (2006).
- [36] H. Alloul, J. Bobroff, M. Gabay, and P. J. Hirschfeld, Defects in correlated metals and superconductors, *Rev. Mod. Phys.* **81**, 45 (2009).
- [37] K. J. Franke, G. Schulze, and J. I. Pascual, Competition of superconductivity phenomena and Kondo screening at the nanoscale, *Science* **332**, 940 (2011).
- [38] E. J. H. Lee, X. Jiang, R. Žitko, R. Aguado, C. M. Lieber, and S. De Franceschi, Scaling of subgap excitations in a superconductor-semiconductor nanowire quantum dot, *Phys. Rev. B* **95**, 180502(R) (2017).
- [39] V. Meden, The Anderson-Josephson quantum dot—A theory perspective, *J. Phys.: Condens. Matter* **31**, 163001 (2019).
- [40] S. Shao, K. Zhou, and Z. Zhang, Impurity-induced Shiba bound state in the BCS-BEC crossover regime of two-dimensional fermi superfluid, *Chin. Phys. B* **28**, 070501 (2019).
- [41] R. W. Richardson, A restricted class of exact eigenstates of the pairing-force Hamiltonian, *Phys. Lett.* **3**, 277 (1963).
- [42] R. W. Richardson, Numerical study of the 8-32-particle eigenstates of the pairing Hamiltonian, *Phys. Rev.* **141**, 949 (1966).
- [43] J. von Delft and F. Braun, Superconductivity in ultrasmall grains: Introduction to Richardson’s exact solution, [arXiv:cond-mat/9911058](https://arxiv.org/abs/cond-mat/9911058) (1999).
- [44] J. Dukelsky, S. Pittel, and G. Sierra, Colloquium: Exactly solvable Richardson-Gaudin models for many-body quantum systems, *Rev. Mod. Phys.* **76**, 643 (2004).

- [45] L. Glazman and G. Catelani, Bogoliubov quasiparticles in superconducting qubits, *SciPost Phys. Lect. Notes* **31** (2021).
- [46] G. Ortiz and J. Dukelsky, BCS-to-BEC crossover from the exact BCS solution, *Phys. Rev. A* **72**, 043611 (2005).
- [47] S. R. White, Density Matrix Formulation for Quantum Renormalization Groups, *Phys. Rev. Lett.* **69**, 2863 (1992).
- [48] U. Schollwöck, The density-matrix renormalization group in the age of matrix product states, *Ann. Phys.* **326**, 96 (2011).
- [49] G. M. Crosswhite, A. C. Doherty, and G. Vidal, Applying matrix product operators to model systems with long-range interactions, *Phys. Rev. B* **78**, 035116 (2008).
- [50] L. Pavešić, D. Bauernfeind, and R. Žitko, Subgap states in superconducting islands, *Phys. Rev. B* **104**, L241409 (2021).
- [51] L. Pavešić and R. Žitko, Qubit based on spin-singlet Yu-Shiba-Rusinov states, *Phys. Rev. B* **105**, 075129 (2022).
- [52] J. C. E. Saldaña, A. Vekris, L. Pavešić, P. Krogstrup, R. Žitko, K. Grove-Rasmussen, and J. Nygård, Excitations in a superconducting Coulombic energy gap, *Nat. Commun.* **13**, 2243 (2022).
- [53] See Supplemental Material at <http://link.aps.org/supplemental/10.1103/PhysRevB.106.024513> for Mathematica notebooks with proofs of the mathematical statements made in this work, DMRG solver input file for the case of flat-band superconductor, as well as the corresponding Mathematica notebook with an exact calculation of the ground state properties.
- [54] R. Žitko, L. Pavešić, and D. Bauernfeind, >QD-SI DMRG solver, *Zenodo* (2022).
- [55] B. T. Matthias, H. Suhl, and E. Curenzwit, Spin Exchange in Superconductors, *Phys. Rev. Lett.* **1**, 92 (1958).
- [56] P. W. Anderson, Localized magnetic states in metals, *Phys. Rev.* **124**, 41 (1961).
- [57] T. Soda, T. Matsuura, and Y. Nagaoka,  $s$ - $d$  exchange interaction in a superconductor, *Prog. Theor. Phys.* **38**, 551 (1967).
- [58] F. Braun and J. von Delft, Superconductivity in ultrasmall metallic grains, *Phys. Rev. B* **59**, 9527 (1999).
- [59] K. Satori, H. Shiba, O. Sakai, and Y. Shimizu, Numerical renormalization group study of magnetic impurities in superconductors, *J. Phys. Soc. Jpn.* **61**, 3239 (1992).
- [60] O. Sakai, Y. Shimizu, H. Shiba, and K. Satori, Numerical renormalization group study of magnetic impurities in superconductors. II. Dynamical excitations spectra and spatial variation of the order parameter, *J. Phys. Soc. Jpn.* **62**, 3181 (1993).
- [61] T. Yoshioka and Y. Ohashi, Ground state properties and localized excited states around a magnetic impurity described by the anisotropic  $s$ - $d$  interaction in superconductivity, *J. Phys. Soc. Jpn.* **67**, 1332 (1998).
- [62] T. Yoshioka and Y. Ohashi, Numerical renormalization group studies on single impurity Anderson model in superconductivity: A unified treatment of magnetic, nonmagnetic impurities, and resonance scattering, *J. Phys. Soc. Jpn.* **69**, 1812 (2000).
- [63] J. Bauer, A. Oguri, and A. C. Hewson, Spectral properties of locally correlated electrons in a Bardeen-Cooper-Schrieffer superconductor, *J. Phys.: Condens. Matter* **19**, 486211 (2007).
- [64] J.-D. Pillet, P. Joyez, R. Žitko, and M. F. Goffman, Tunneling spectroscopy of a single quantum dot coupled to a superconductor: From Kondo ridge to Andreev bound states, *Phys. Rev. B* **88**, 045101 (2013).
- [65] J. C. Estrada Saldaña, A. Vekris, G. Steffensen, R. Žitko, P. Krogstrup, J. Paaske, K. Grove-Rasmussen, and J. Nygård, Supercurrent in a Double Quantum Dot, *Phys. Rev. Lett.* **121**, 257701 (2018).
- [66] S. Kezilebieke, R. Žitko, M. Dvorak, T. Ojanen, and P. Liljeroth, Observation of coexistence of Yu-Shiba-Rusinov states and spin-flip excitations, *Nano Lett.* **19**, 4614 (2019).
- [67] C. Rubio-Verdú, J. Zaldívar, R. Žitko, and J. I. Pascual, Coupled Yu-Shiba-Rusinov States Induced by a Many-Body Molecular Spin on a Superconductor, *Phys. Rev. Lett.* **126**, 017001 (2021).
- [68] D. J. Luitz and F. F. Assaad, Weak-coupling continuous-time quantum Monte Carlo study of the single impurity and periodic Anderson models with  $s$ -wave superconducting baths, *Phys. Rev. B* **81**, 024509 (2010).
- [69] M. Žonda, V. Pokorný, V. Janiš, and T. Novotný, Perturbation theory of a superconducting  $0$ - $\pi$  impurity quantum phase transition, *Sci. Rep.* **5**, 8821 (2015).
- [70] V. Pokorný and M. Žonda, Correlation effects in superconducting quantum dot systems, *Phys. B: Condens. Matter* **536**, 488 (2018).
- [71] T. Domański, M. Žonda, V. Pokorný, G. Górski, V. Janiš, and T. Novotný, Josephson-phase-controlled interplay between correlation effects and electron pairing in a three-terminal nanostructure, *Phys. Rev. B* **95**, 045104 (2017).
- [72] P. Zalom, V. Pokorný, and T. Novotný, Spectral and transport properties of a half-filled anderson impurity coupled to phase-biased superconducting and metallic leads, *Phys. Rev. B* **103**, 035419 (2021).
- [73] S. M. A. Rombouts, K. Van Houcke, and L. Pollet, Loop Updates for Quantum Monte Carlo Simulations in the Canonical Ensemble, *Phys. Rev. Lett.* **96**, 180603 (2006).
- [74] E. A. Yuzbashyan, A. A. Baytin, and B. L. Altshuler, Strong-coupling expansion for the pairing Hamiltonian for small superconducting metallic grains, *Phys. Rev. B* **68**, 214509 (2003).
- [75] J. R. Schrieffer and P. A. Wolff, Relation between the Anderson and Kondo Hamiltonians, *Phys. Rev.* **149**, 491 (1966).
- [76] B. W. Heinrich, J. I. Pascual, and K. J. Franke, Single magnetic adsorbates on  $s$ -wave superconductors, *Prog. Surf. Sci.* **93**, 1 (2018).
- [77] P. Ring and P. Schuck, *The Nuclear Many-body Problem* (Springer-Verlag, New York, 1980).
- [78] A. Kerman, Pairing forces and nuclear collective motion, *Ann. Phys.* **12**, 300 (1961).
- [79] P. V. Isacker, K. B. Wolf, L. Benet, J. M. Torres, and P. O. Hess, Seniority in quantum many-body systems, in *AIP Conference Proceedings* (AIP, College Park, MD, 2010).
- [80] V. A. Khodel and V. R. Shaginyan, Superfluidity in system with fermion condensate, *JETP Lett.* **51**, 488 (1990).
- [81] G. E. Volovik, Graphite, graphene, and the flat-band superconductivity, *JETP Lett.* **107**, 516 (2018).
- [82] S. Bravyi, D. P. DiVincenzo, and D. Loss, Schrieffer-Wolff transformation for quantum many-body systems, *Ann. Phys.* **326**, 2793 (2011).
- [83] T. Hecht, A. Weichselbaum, J. von Delft, and R. Bulla, Numerical renormalization group calculation of near-gap peaks in spectral functions of the Anderson model with superconducting leads, *J. Phys.: Condens. Matter* **20**, 275213 (2008).
- [84] I. Affleck, J.-S. Caux, and A. M. Zagoskin, Andreev scattering and Josephson current in a one-dimensional electron liquid, *Phys. Rev. B* **62**, 1433 (2000).

- [85] E. Vecino, A. Martín-Rodero, and A. LevyYeyati, Josephson current through a correlated quantum level: Andreev states and Pi-junction behavior, *Phys. Rev. B* **68**, 035105 (2003).
- [86] F. S. Bergeret, A. LevyYeyati, and A. Martín-Rodero, Josephson effect through a quantum dot array, *Phys. Rev. B* **76**, 174510 (2007).
- [87] K. Grove-Rasmussen, G. Steffensen, A. Jellinggaard, M. H. Madsen, R. Žitko, J. Paaske, and J. Nygård, Yu-Shiba-Rusinov screening of spins in double quantum dots, *Nat. Commun.* **9**, 2376 (2018).
- [88] K. Yosida, Bound state due to the  $s$ - $d$  exchange interaction, *Phys. Rev.* **147**, 223 (1966).
- [89] R. Žitko and M. Fabrizio, Non-Fermi-liquid behavior in quantum impurity models with superconducting channels, *Phys. Rev. B* **95**, 085121 (2017).
- [90] F. von Oppen and K. J. Franke, Yu-Shiba-Rusinov states in real metals, *Phys. Rev. B* **103**, 205424 (2021).
- [91] H. Schmid, J. F. Steiner, K. J. Franke, and F. von Oppen, Quantum Yu-Shiba-Rusinov dimers, *Phys. Rev. B* **105**, 235406 (2022).